

Uremic Solute-Aryl Hydrocarbon Receptor-Tissue Factor Axis Associates with Thrombosis after Vascular Injury in Humans

Vijaya B. Kolachalama ^{1,2,3} Moshe Shashar,⁴ Faisal Alousi,⁴ Sowmya Shivanna,⁴ Keshab Rijal,⁴ Mostafa E. Belghasem ⁵ Joshua Walker,⁴ Shinobu Matsuura,² Gary H. Chang,¹ C. Michael Gibson,⁶ Laura M. Dember ⁷ Jean M. Francis,⁴ Katya Ravid ² and Vipul C. Chitalia ^{2,4,5}

¹Section of Computational Biomedicine and ⁴Renal Section, Department of Medicine, ²Department of Medicine, Whitaker Cardiovascular Institute, and ⁵Department of Pathology and Laboratory Medicine, Boston University School of Medicine, Boston, Massachusetts; ³Hariri Institute for Computing and Computational Science and Engineering, Boston University, Boston, Massachusetts; ⁶Cardiovascular Medicine, Department of Medicine, Beth Israel Deaconess Medical Center, Harvard Medical School, Boston, Massachusetts; and ⁷Renal-Electrolyte and Hypertension Division, Department of Medicine, Center for Clinical Epidemiology and Biostatistics, Department of Biostatistics, Epidemiology and Informatics, Perelman School of Medicine at the University of Pennsylvania, Philadelphia, Pennsylvania

ABSTRACT

Individuals with CKD are particularly predisposed to thrombosis after vascular injury. Using mouse models, we recently described indoxyl sulfate, a tryptophan metabolite retained in CKD and an activator of tissue factor (TF) through aryl hydrocarbon receptor (AHR) signaling, as an inducer of thrombosis across the CKD spectrum. However, the translation of findings from animal models to humans is often challenging. Here, we investigated the uremic solute–AHR–TF thrombosis axis in two human cohorts, using a targeted metabolomics approach to probe a set of tryptophan products and high-throughput assays to measure AHR and TF activity. Analysis of baseline serum samples was performed from 473 participants with advanced CKD from the Dialysis Access Consortium Clopidogrel Prevention of Early AV Fistula Thrombosis trial. Participants with subsequent arteriovenous thrombosis had significantly higher levels of indoxyl sulfate and kynurenine, another uremic solute, and greater activity of AHR and TF, than those without thrombosis. Pattern recognition analysis using the components of the thrombosis axis facilitated clustering of the thrombotic and nonthrombotic groups. We further validated these findings using 377 baseline samples from participants in the Thrombolysis in Myocardial Infarction II trial, many of whom had CKD stage 2–3. Mechanistic probing revealed that kynurenine enhances thrombosis after vascular injury in an animal model and regulates thrombosis in an AHR-dependent manner. This human validation of the solute–AHR–TF axis supports further studies probing its utility in risk stratification of patients with CKD and exploring its role in other diseases with heightened risk of thrombosis.

J Am Soc Nephrol 29: 1063–1072, 2018. doi: <https://doi.org/10.1681/ASN.2017080929>

Thrombosis is a frequent and serious complication of vascular interventions such as surgery or endovascular procedures.¹ CKD increases the risk of vascular injury–associated thrombosis by 6.5–10-fold.^{2–7} Currently, serum creatinine concentration and CKD stage serve as generic indicators of thrombosis risk factor.⁸ Risk stratification using a broader set of mechanistically driven biomarkers is

Received August 24, 2017. Accepted December 21, 2017.

Published online ahead of print. Publication date available at www.jasn.org.

Correspondence: Dr. Vipul C. Chitalia, Renal Section, Department of Medicine, Boston University Medical Center, Evans Biomedical Research Center, X-530, Boston, MA 02118. E-mail: vichital@bu.edu or vipul.chitalia@bmc.org

Copyright © 2018 by the American Society of Nephrology

likely to improve thrombosis risk prediction and improve antithrombotic management of patients with CKD.

The role of retained solutes (uremic solutes) in enhancing thrombogenicity of the CKD milieu (uremia) has been demonstrated in *ex vivo* models and recently in mouse models.^{9–12} Particularly, indolic solutes, such as indoxyl sulfate (IS) produced by tryptophan metabolism and retained starting in the early stages of CKD, increase tissue factor (TF) expression in the vessel wall to trigger thrombosis¹⁰ through aryl hydrocarbon receptor (AHR) signaling, thereby defining the uremic solute–AHR–TF thrombosis pathway.^{11,13} Although these studies established a mechanistic basis for this pathway and its potential druggability,^{9,11} validation of these findings in humans has yet to be performed.

Here, we set out to comprehensively examine the uremic solute–AHR–TF axis in patients from two clinical trials that focused on thrombosis after different types of vascular injury. The Dialysis Access Consortium Clopidogrel Prevention of Early AV Fistula Thrombosis trial (DAC-Fistula)¹⁴ and the Thrombolysis in Myocardial Infarction (TIMI)–II study¹⁵ examined the thrombotic complications after hemodialysis arteriovenous fistula (AVF) creation and balloon angioplasty, respectively. Although these two types of injury models are distinct, their postinjury vascular beds share common characteristics including endothelial damage and exposure of vascular smooth muscle cells (vSMCs), both of which contribute to thrombosis.^{16–18} Using this mechanistic rationale, this study leverages a prevalidated liquid chromatography–mass spectrometry (LC/MS)–based targeted metabolomics analysis,¹⁹ and high-throughput AHR and TF activity assays in thrombosis-relevant cells¹¹ to evaluate the abilities of sera obtained before enrollment to increase AHR signaling and TF activity. The DAC-Fistula trial randomized 877 patients with ESRD to clopidogrel or placebo with the primary outcome of AVF thrombosis within 6 weeks of its creation, which occurred in 137 (15%) participants.^{14,20} Given outcome of

Significance Statement

CKD is a strong risk factor for thrombosis. Previously, animal studies have shown that uremic solutes mediate this event through the activation of Aryl Hydrocarbon Receptor (AHR) and tissue factor (TF), thus, defining a uremic thrombosis axis. In this study, its human relevance is examined using data collected from two distinct clinical trials. In line with the animal studies, the analysis on 850 sera samples showed a significant correlation of a set of uremic solutes, AHR and TF activities with the thrombotic events. This human validation supports further studies to explore this novel axis as a uremic thrombosis biomarker and to test its contribution in other diseases characterized by thrombosis.

post-vascular injury thrombosis,²¹ the results obtained from analysis of the DAC-Fistula were validated in a subgroup of patients (*n*=377) from the TIMI-II trial who underwent percutaneous transluminal coronary angioplasty (PTCA) (*n*=1144) for ST-segment elevation myocardial infarction.¹⁵ Reinfarction or reocclusion of the coronary vessel in these patients was considered as a post-PTCA thrombotic “event” (9.8% of 377 participants). In this study, all of the sera samples were probed for a set of solutes, which are associated with tryptophan metabolism (such as IS) and retained in patients with CKD.^{22,23} This set included indole acetic acid (IA), L-kynurenine (Kyn) and ynurenic acid (KA), anthranilic acid (AA), and xanthurenic acid (XA).¹⁹

RESULTS

Solute-AHR-TF Axis in AVF Thrombosis

A comprehensive analysis of components of the uremic solutes–AHR–TF axis (Figure 1, Supplemental Figure 1, A–C) in the samples from the DAC fistula trial was performed with the hypothesis that the components of this axis are likely to be higher in patients with AVF thrombosis. Because biosample collection was not initiated until approximately half of the trial

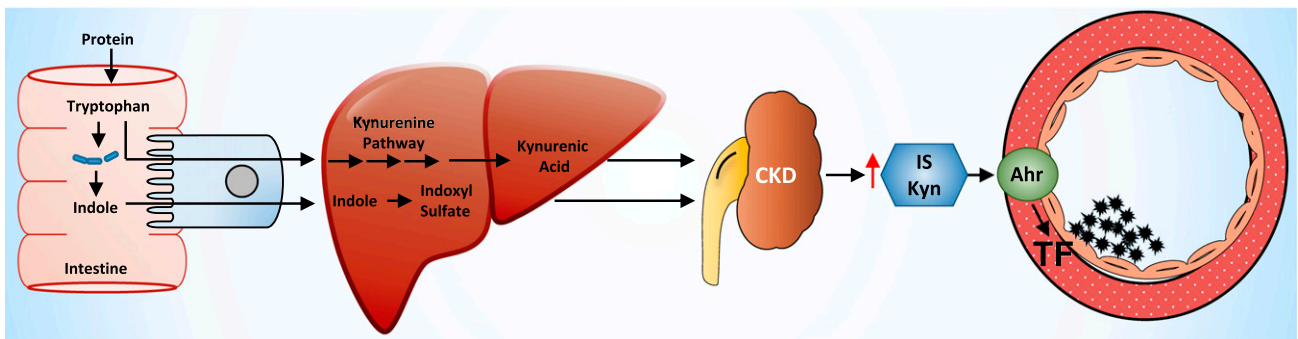


Figure 1. Uremic thrombosis axis (uremic solutes–AHR–TF) in humans. Working hypothesis of the uremic thrombosis axis: Tryptophan degraded to indole by intestinal bacteria undergoes conversion to indolic solutes such as IS in the liver. Tryptophan absorbed through the portal circulation also undergoes metabolism in the liver to Kyn. IS and Kyn are retained in patients with CKD and their elevated levels activate the AHR pathway to increase TF levels in the vessel wall to enhance thrombosis. The uremic solutes–AHR–TF axis is a novel and CKD-specific thrombotic signaling pathway.

Table 1. Baseline characteristics of DAC-Fistula trial participants

Study/Baseline Characteristics ^a	DAC-Fistula Trial (n=470)		
	Thrombosis Group (n=60)	Nonthrombosis Group (n=410)	P Value
Age, yr ^b	54.69 (15.85)	52.35 (13.88)	0.28
Male	33 (55.0%)	278 (67.8%)	0.06
BMI, kg/m ^{2b}	29.76 (8.20)	30.02 (8.49)	0.82
Black	32 (53.3%)	202 (49.3%)	0.58
BP, mmHg ^b			
Systolic	138 (20.77)	140 (21.28)	0.48
Diastolic	77 (14.80)	79 (13.30)	0.38
Diabetes mellitus	30 (50.0%)	208 (50.7%)	1.00
Cardiovascular diseases	11 (18.3%)	90 (21.9%)	0.62
Cerebrovascular diseases	3 (5.0%)	28 (6.8%)	0.78
Venous thromboembolism disease	3 (5.0%)	11 (2.7%)	0.40
Aspirin use	47 (78.3%)	337 (82.2%)	0.48
Clopidogrel use	22 (36.7%)	203 (49.5%)	0.07
Statin use	19 (31.7%)	108 (26.3%)	0.44
Hemoglobin, g/dl ^b	11.70 (2.07)	11.53 (1.90)	0.56
Serum albumin, g/dl ^b	3.70 (0.64)	3.73 (0.63)	0.75
Number of patients on HD before enrollment	39 (65.0%)	240 (58.5%)	0.40
Creatinine in patients on HD, mg/dl ^b	8.32 (3.98)	8.80 (3.73) ^c	0.48
Fistula location			
Forearm	38 (63.3%)	212 (51.7%)	0.09
Upper arm	22 (36.6%)	198 (48.2%)	0.09

BMI, body mass index; HD, hemodialysis.

^aThis is the subgroup of DAC-Fistula trial participants for whom baseline blood samples were collected.

^bMean (SD).

^cCreatinine data from only 238 subjects was available.

participants were enrolled, baseline sera (before fistula creation) were available from only 473 participants. Because our focus was on identifying markers of thrombosis regardless of its time of occurrence, we included all AVF thrombosis events in this trial. The baseline characteristics of participants were similar between the thrombotic “event” and the nonthrombotic “no-event” groups (Table 1).

We first compared the distribution of the components of the solute-AHR-TF axis between event and no-event groups (Table 1). Among analyzed metabolites, IS, Kyn, and kynurenic acid showed a nonoverlapping distribution between both the groups and significantly higher levels ($P<0.001$) in the event group (Figure 2, A–D, Supplemental Figure 2A), whereas no differences were observed for other metabolites, including IA (Figure 2, E–F, Supplemental Figure 2, B and C). Similar differences in the distribution and higher levels of AHR activity were observed in the event group (Figure 2, G and H). Given the potential contribution of vSMCs and endothelial cells to AVF thrombosis, TF activities were analyzed in both these cell types. The results showed significantly higher TF activity in both of in the event group (Figure 2, I–K). Furthermore, significant correlations between IS-AHR ($R^2=0.59$, $P<0.001$), Kyn-AHR ($R^2=0.51$, $P<0.001$), and IS-TF ($R^2=0.24$, $P<0.05$) were noted only in the event group.

One of the central expectations of identifying a biomarker signature is to determine a potential set of molecules

that associates with a process and differentiates patients on the basis of risk. We employed data clustering techniques that are part of the broad field of machine learning,^{24–26} to discern the discriminatory potential of the parameters of the solute-AHR-TF axis to segregate patients with events. For example, methods such as principal component analysis (PCA) (Figure 2L) allowed us to fully appreciate the cumulative effect of the components of the thrombosis axis by reducing such high-dimensional data to fewer dimensions without significant loss of information.^{25,27} The underlying hypothesis is that patients with thrombosis will be clustered together and away from the group with no thrombosis. PCA showed that the first two principal components plotted on a two dimensional (2D) map revealed a distinct separation between the “event” and “no-event” subgroups, and this clustering was also evident using several other dimensionality reduction methods (Supplemental Figure 2, D–F). Taken together, these results indicate that the combination of uremic metabolites, AHR, and TF can segregate the study participants with and without thrombosis, thus supporting their biomarker potential.

Validation of the Solute-AHR-TF Axis in the TIMI-II Study Cohort

We substantiated our findings of increased levels of solutes, AHR, and TF activities in patients with post-vascular injury thrombosis using another clinical cohort, the TIMI-II trial (Supplemental Figure 1D). Sera samples ($n=377$) were

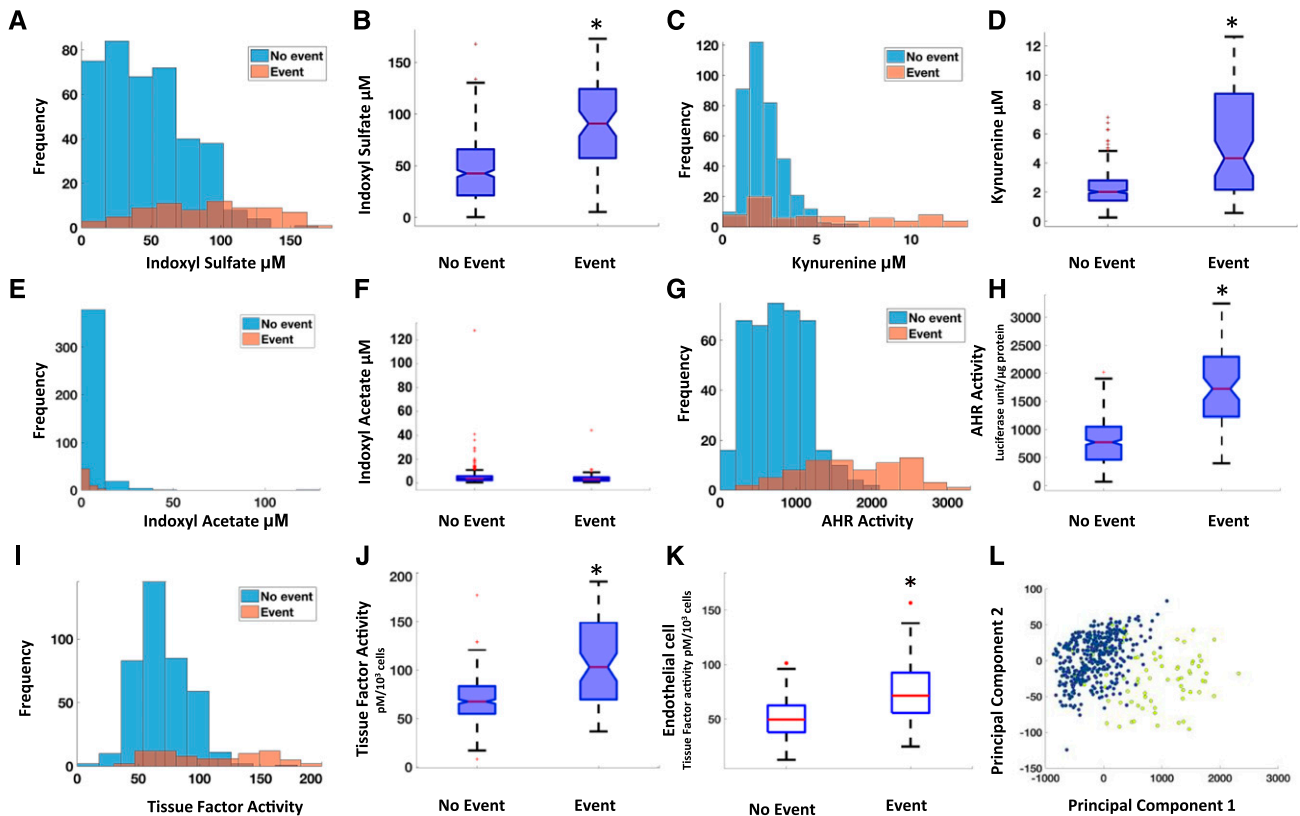


Figure 2. Increased levels of IS, Kyn, and AHR and TF activities in patients with AVF thrombosis in DAC-Fistula trial. (A, C, E, G, and I) Histograms of the metabolites as well as the functional activities of the proteins between the AVF thrombosis “event” (as defined in the text) and “no-event” groups are shown. The concentrations of metabolites are in micromolars and AHR and TF activities are in luciferase units/ μg protein and $\text{pM}/10^3$ cells, respectively. (B, D, F, H, and J) Box plot visualization of the thrombosis “event” and “no-event” groups for the measured indicators in the DAC-Fistula trial. The lines in red in the boxes represent median levels of the measured indicator (metabolite or the level of activity). The lower and upper boundaries of the boxes represent the 25th and 75th percentiles, respectively. The lower and upper whiskers represent the minimum and maximum values, respectively. Note that statistically significant differences ($P < 0.001$) were observed between the “event” and “no-event” groups for each case other than IA. (K) Box plot showing the endothelial cell TF activity for the “event” and “no-event” groups ($P < 0.001$). (L) PCA on the components of the thrombosis axis was performed and the first two principal components capturing a major portion of the total variance of the original measurements are shown. The subjects belonging to the “event” group are shown in yellow and those in the “no-event” group are shown in blue. * P -value significant.

obtained from patients who underwent PTCA ($n=1144$). Of 377 patients, 66% had CKD stage 2 or 3 (Supplemental Figure 3A). Complications, such as postangioplasty protocol lesion thrombosis, nonprotocol lesion thrombosis, occlusion of infarct-related vessel, and occlusion of branch(es) of infarct-related vessels, were all grouped as thrombotic events ($n=37$). Baseline characteristics were similar in the participants with and without events (Table 2).

Among examined metabolites, Kyn and XA showed differences in the distribution pattern between event and no-event groups and significantly higher levels (Kyn $P < 0.001$ and XA $P = 0.03$) in the event group (Figure 3, A and B, Supplemental Figure 3A). Other metabolites including IS did not show any differences between the event and no-event groups (Figure 3, C and D, Supplemental Figure 3, B–E). Significantly higher

AHR and TF activities were noted in the event group (Figure 3, E–H). Using levels of Kyn, AHR, and TF activities, the PCA performed on the TIMI-II data showed a distinct separation between the “event” and “no-event” patient groups (Figure 3I, Supplemental Figure 3, F–H), indicating the presence of a crossplatform signature (metabolite and cell activities) associated with the post-vascular interventional thrombosis.

Kyn Mediates Thrombosis through AHR-TF Axis

Although the association of Kyn with the blood levels of TF is known,²² its exact mechanism or relevance to the post-vascular injury thrombosis remains poorly understood. The data from both the cohorts showed significantly higher levels of Kyn in the event group; we therefore hypothesized that Kyn may enhance thrombosis after vascular injury. We first probed

Table 2. Baseline characteristics of TIMI-II trial participants included in this study

Study/Baseline Characteristics	TIMI-II (n=377)		P Value
	Thrombosis Group (n=35)	Control Group (n=342)	
Age, yr ^a	57.26 (9.85)	55.26 (10.27)	0.26
Male	28 (80.0%)	274 (80.1%)	>0.99
Black	2 (5.7%)	30 (8.8%)	0.75
Body mass index, kg/m ^{2a}	27.97 (4.11)	27.09 (4.77)	0.84
BP, mmHg ^a			
Systolic	128 (19.00)	128 (21.55)	0.97
Diastolic	80 (12.28)	80 (13.63)	0.46
Diabetes mellitus	1 (2.8%)	43 (12.5%)	0.10
Hypertension	13 (37.1%)	125 (36.6%)	>0.99
Angina pectoris	18 (51.4%)	192 (56.1%)	0.60
Congestive heart failure	1 (2.9%)	5 (1.5%)	0.45
Previous myocardial infarction	4 (11.4%)	37 (10.8%)	0.78
Peripheral vascular disease	1 (2.9%)	10 (2.9%)	>0.99
Serum creatinine, mg/dl ^a	1.14 (0.26) ^b	1.12 (0.25) ^c	0.66
eGFR, (ml/min per 1.73 m ²) CKD-EPI formula ^a	74.86 (17.60)	74.73 (17.63)	0.97
Aspirin	5 (14.3%)	48 (14.0%)	>0.99
Dipyridamole	0 (0%)	3 (0.88%)	>0.99
Heparin	1 (2.9%)	6 (1.8%)	0.49
Other anticoagulants	0 (0%)	0 (0%)	>0.99

CKD-EPI, Chronic Kidney Disease Epidemiology Collaboration. The data are displayed as number (percentage of total group).

^aMean (SD).

^bCreatinine values available in 31 subjects.

^cCreatinine values available in 325 subjects.

the mechanism of Kyn's prothrombotic activity through the AHR-TF axis, considering earlier reports showing Kyn to be a ligand for AHR in other cell types^{28,29} and our own findings of AHR upregulating TF expression.¹¹ We examined AHR signaling and TF in primary human aortic vSMCs in response to a wide range of Kyn concentrations. We observed a dose-dependent increase in AHR activity and TF expression and activity with increasing concentration of Kyn, all of which were suppressed by a specific AHR inhibitor (CH223191)³⁰ (Figure 4, A–C). These data indicate that Kyn at the concentrations observed in patients with CKD activates AHR signaling to upregulate TF.

To evaluate the effect of Kyn on vascular injury–associated thrombosis *in vivo*, we generated a novel animal model wherein carotid artery thrombosis was examined in the milieu of elevated Kyn levels. Kyn levels were elevated in these animals by injecting Kyn and simultaneously blocking its excretion using probenecid, as done for other uremic solutes.^{9,31} This protocol and dosage yielded serum Kyn concentrations comparable to those observed in humans with ESRD³² (Figure 4D). The animals were subjected to the carotid artery ferric chloride (FeCl₃) injury model, a standard model of post-vascular injury thrombosis.³³ The drop in carotid artery blood flow to baseline (time to occlusion, TtO) as detected in real-time with an ultrasound probe served as an end point of the study (Figure 4E).⁹ There was a significant reduction in TtO in the Kyn group compared with the controls, and TtO improved significantly with CH223191. These data indicate that Kyn

enhances postinjury thrombosis in an AHR-dependent manner (Figure 4F).

DISCUSSION

Markers of thrombosis currently used in clinical practice do not include the disease-specific risk factors or the vessel wall mediators critical to thrombosis after vascular injury. We have performed a comprehensive analysis that elucidates the nodes of a thrombosis axis at the intersection of endogenous metabolites and vessel wall factors. These findings, along with previous observations in other models,^{11,13} underscore the importance of the uremic solute–AHR–TF axis as a potential marker of thrombosis in humans. We found higher blood concentrations of Kyn in the thrombosis groups from both the DAC-Fistula and TIMI-II trial cohorts, and higher blood levels of IS in the thrombosis group of the DAC-Fistula trial cohort. Importantly, we uncovered Kyn as regulator of TF through AHR. Further, we demonstrate higher AHR and TF activities in patients with thrombosis in both trials. Pattern recognition analysis highlighted the biomarker potential of this thrombosis axis.

Circulating metabolites are often associated with clinical events.^{34–36} However, the current work differentiates itself from such studies. First, in addition to metabolites, nodes of the signaling axis—the ligand (uremic solutes), the mediator (AHR signaling), and the effector molecule (TF)—were correlated to thrombosis. Second, the results from both the trials

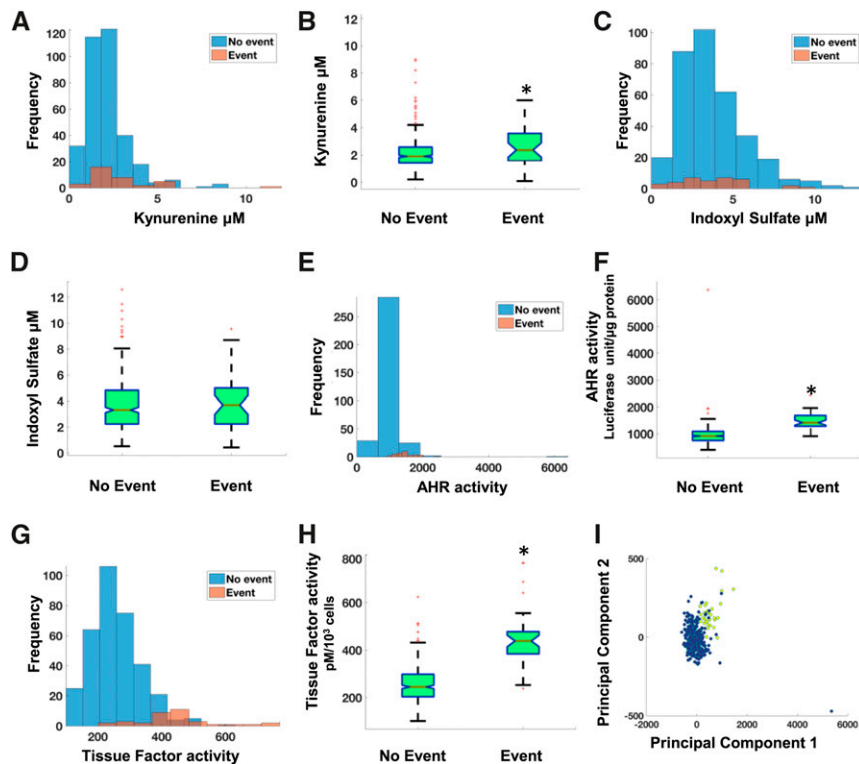


Figure 3. Increased levels of Kyn and AHR and TF activities in patients with postangioplasty thrombosis in TIMI-II trial. (A, C, E, and G) Histograms of the metabolites as well as the functional activities of the proteins show distinct differences between the thrombotic “event” and “no-event” groups. The concentrations of metabolites are in micromolar and AHR and TF activities are in luciferase units/ μg protein and TF activity $\text{pM}/10^3$ cells, respectively. (B, D, F, and H) Box plot visualization of the thrombosis “event” and “no-event” groups for the measured indicators in the TIMI-II trial. Statistically significant differences ($P < 0.001$) were observed between the “event” and “no-event” groups for each case. (I) First two principal components capturing a major portion of the total variance of the original data are shown. The patients belonging to the thrombotic “event” group are shown in yellow and ones in the “no-event” group are shown in blue. *P-value significant.

uncovered previously unknown association of Kyn through the AHR-TF axis to post-vascular injury thrombosis, which was further supported in a new animal model (Figure 4, D and E). In so doing, it also provided a mechanistic rationale to previous epidemiologic studies that linked Kyn to cardiovascular diseases in patients both with CKD and without CKD^{37–39} and to other reports of TF and AHR as mediators of atherothrombotic disease.^{40–42}

Thrombosis after Vascular Surgery

Although the clopidogrel-treated group showed overall reduced AVF thrombosis compared with the placebo-treated group in the DAC-Fistula trial,^{14,20} 12% of patients still experienced AVF thrombosis. Our subgroup analysis of clopidogrel-treated individuals with thrombosis revealed significantly higher levels of AHR and TF activities as well as uremic solutes compared with the nonthrombosis group (Supplemental Figure 4). This implies that even with an antiplatelet regimen, observed thrombotic events were perhaps triggered due to other signaling pathways. The uremic thrombosis axis represents such a pathway, which warrants further exploration in patients with CKD experiencing thrombosis despite being on

antiplatelet therapy. The DAC-Fistula study did not show an increase in IA in the event group, whereas IS was significantly higher in patients with AVF thrombosis. This observation suggests that not all indolic solutes are the same and that IS and IA may have divergent roles.

The study of TF activity in endothelial cells has implications for other models of thrombosis. Venous thrombosis occurs on the dysfunctional endothelial monolayer.⁴³ The increase in the endothelial cell TF activity in the thrombosis group in patients with advanced CKD/ESRD may suggest contribution of the uremic thrombosis axis to the pathogenesis of venous thromboembolism. This may also explain CKD/ESRD as a risk factor for venous thromboembolism (incidence in normal renal function 66 of 100,000 patients versus ESRD 527 of 100,000 patients).^{44,45}

Postangioplasty Thrombosis

Although the TIMI-II study was conducted two decades ago, the findings from that trial are relevant currently because the nature of vascular injury and the postinterventional bed remain similar, with the current standard-of-care treatments such as PTCA followed by stenting.

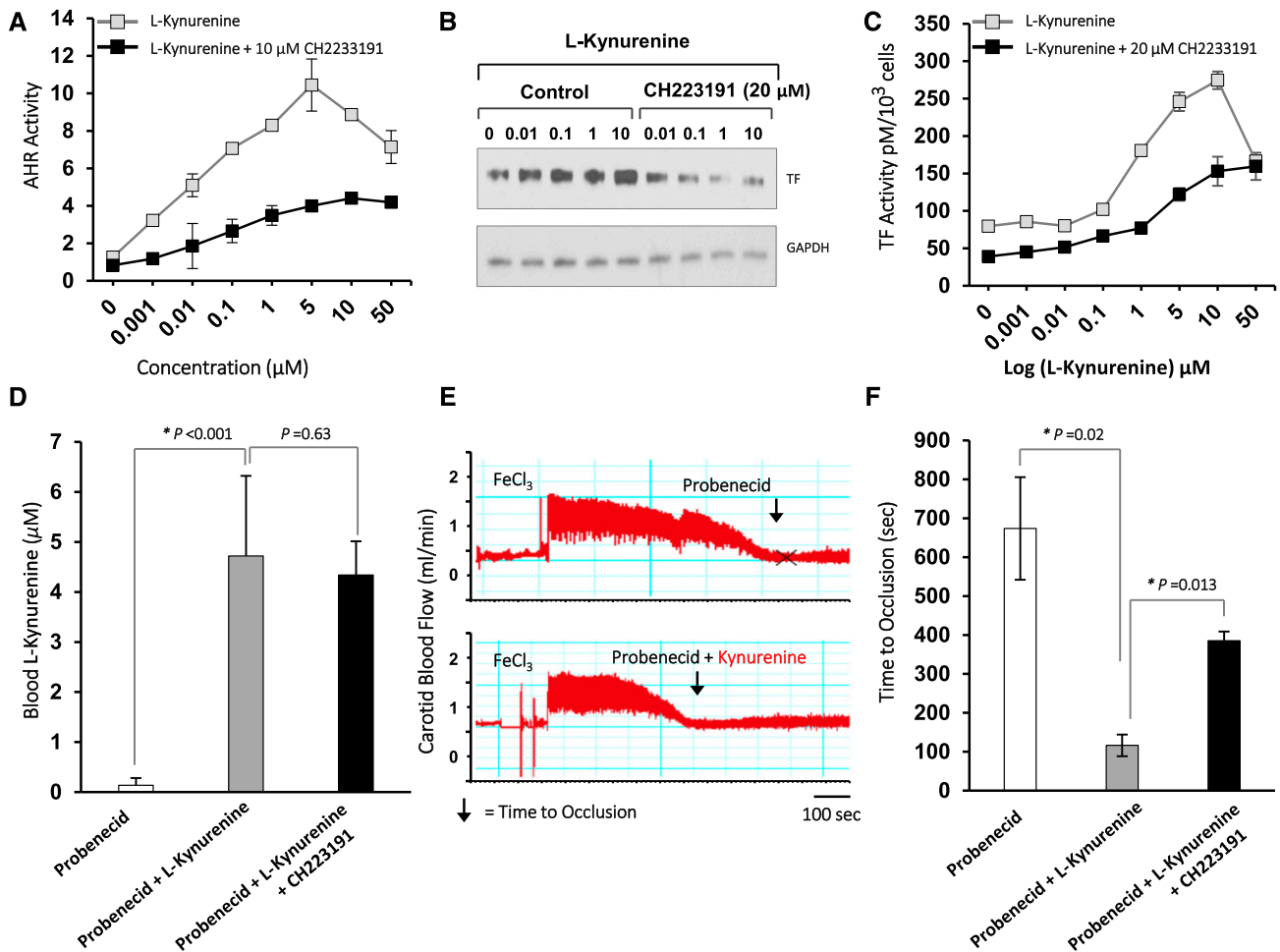


Figure 4. Kyn regulates thrombosis through the AHR-TF axis. (A) Kyn activates AHR signaling in primary human aortic vSMCs. vSMCs stably expressing a xenobiotic responsive element promoter–luciferase reporter construct were treated with Kyn at levels corresponding to different CKD stages and an AHR antagonist CH2233191 (10 μ M) for 24 hours. AHR activity was quantified by firefly luciferase units and normalized to protein content of the cells. An average of three independent experiments performed in duplicate is shown. Compared with control, *P* values for different Kyn concentrations were *P*=0.03 for 0.001 μ M, *P*=0.001 for 0.01 μ M, and *P*<0.001 for all of the other concentrations of Kyn. Compared with Kyn+CH2233191-treated samples, *P* values were <0.001 for all of the points. Error bars=SD. (B) AHR antagonist suppresses Kyn-induced TF expression. vSMCs treated with the indicated concentrations of Kyn with or without 20 μ M CH2233191 for 24 hours. The lysates were probed for TF. GAPDH served as a loading control. A representative of three independent experiments is shown. (C) Kyn induces procoagulant TF activity in an AHR-dependent manner. vSMCs were treated with indicated concentrations of Kyn with or without 20 μ M CH2233191 for 24 hours and TF activity was measured and normalized to total number of viable cells and expressed as pM/10³ cells. An average of TF activity performed in three independent experiments done in duplicate is shown. Error bars=SD. Compared with the control (Kyn=0 μ M), the *P* values were *P*=0.01 for Kyn of 1 μ M and *P*<0.001 for Kyn concentrations of 10 and 100 μ M. A significant reduction in TF activity was noted at all of the concentrations of Kyn from 0.001 to 10 μ M with CH2233191 (*P*=0.001 for Kyn from 0.001 to 5 μ M and *P*=0.03 for Kyn 10 μ M). (D) Generation of Kyn levels equivalent to levels found in patients with ESRD. Blood samples collected from animals exposed to a combination of probenecid and Kyn were analyzed using LC/MS. Probenecid-injected animals served as controls. An average of Kyn levels from five animals at the end of 4 days of exposure and before thrombosis assay is shown. The *P* value corresponds to a significant increase in serum Kyn levels in the probenecid+Kyn group compared with the probenecid group alone. Error bar=SD. (E) The pattern of carotid artery blood flow with occlusion due to thrombus is shown. An ultrasound probe measured carotid artery flow in five C57BL/6 animals and was noted to be 1.25–2 ml/min. The flow was monitored for 20 minutes after the application of 10% FeCl₃ strip. The time till the blood flow dropped to baseline was considered as TtO and is depicted by an arrow. A representative carotid artery blood flow pattern is shown from five animals in each group. (F) Kyn enhances thrombogenicity in an AHR-dependent manner. The TtO was compared within two groups after 5 days of exposure to different agents. An average of TtO from five animals is shown. A significant reduction in TtO with Kyn was noted. Error bars=SD.

Differences in the metabolomics patterns between two trials may point to specific mechanisms of solute elevation. In contrast to the DAC-Fistula trial, IS levels were not higher in the thrombotic group of the TIMI-II cohort (Figure 3D). Unlike the DAC-Fistula cohort (consisting of patients with CKD stage 5 and ESRD), the TIMI-II cohort had lower levels of IS, because it consisted of subjects with CKD stage 2 or 3 (66%) and none with ESRD. Although the level of IS corresponding to CKD stage 2–3 in vSMCs doubled TF levels in a previous study,¹¹ this discrepancy between the cell-based model and human data warrants further investigation. Higher levels of Kyn were observed in the thrombotic group without any differences in renal function in the TIMI-II cohort (Table 2). This result implicates factors other than reduced excretion. In line with the complex multistep metabolism of Kyn, it is likely that the levels of Kyn may be influenced by factors including dietary composition, microbiome, and metabolic enzymes, *etc.*^{32,46,47} Furthermore, inflammation, oxidative stress, and endothelial dysfunction, all of which are increased in the setting of acute coronary syndrome, can also increase Kyn in blood.⁴⁸

Enhanced TF levels in the vessel wall induced by solute-AHR signaling triggering the extrinsic coagulation pathway to generate thrombin in blood may have therapeutic implications. Although traditionally anticoagulants and antiplatelet agents are used for venous and arterial thrombosis, respectively,¹ our current data support targeting either the CKD-specific thrombosis axis and/or the thrombin-based anticoagulants to suppress the extrinsic coagulation cascade downstream of TF activation, especially in patients with CKD, for effective antithrombosis after vascular intervention.

Pattern Recognition

Unsupervised clustering is a part of machine learning that is commonly used to cluster data that have several dimensions. Many of these methods also allow for dimensionality reduction which then facilitates data visualization,^{24–27} while retaining the same level of information but in an embedded form. When these reduced dimensions are visualized on a 2D plot, potential clustering/grouping of patients on the basis of their event status can be observed. For example, in our study, independent processing of the datasets using four pattern recognition techniques resulted in distinct clustering of the “event” group. These data suggest the solute-AHR-TF pathway as a candidate biomarker signature for thrombosis after vascular injury in patients with CKD. However, sufficiently powered prospective studies are warranted to validate the components of the uremic axis before being considered for clinical use.

Study Limitations

Because of limited availability of sera samples, only a subset of the TIMI-II cohort (11%) was analyzed. The TF activity was measured only in vSMC in the TIMI-II study due to inadequate quantity of samples. Both trials allowed analysis of a single sample for the parameters, which are known to fluctuate over time. To fully characterize the hyperthrombotic uremic

milieu, future studies are required with access to larger numbers of samples obtained at multiple time points from cohorts with similar outcomes and preferably with longitudinal follow-up data.⁴⁹ Although the stability of solutes was examined only over a 4-year period (Supplemental Figure 5), the detrimental effect of extended storage especially on TIMI-II samples cannot be ruled out. We did not analyze the free fractions of the solutes, which are considered to be pathogenic.²³ This does not represent a major shortcoming, because studies have demonstrated a high degree of correlation of total solutes with the free fractions⁵⁰ and with overall and cardiovascular mortality in patients at different CKD stages.⁵¹ Caution is warranted in interpreting eGFR values in both the studies. The creatinine assays for both the trials were not calibrated using isotope dilution mass spectrometry, an accurate method of creatinine assay standardization recommended for calculating eGFR equations and comparing creatinine values measured in different laboratories or at different times.⁵²

Because thrombosis remains a common and a potentially fatal complication of vascular interventions, its precise risk estimation is imperative. Our study represents an integrative approach focused on probing the disease-specific risk mediators *via* mechanistic studies at biochemical and computational levels, such as machine learning–based analysis, in human cohorts. Such an approach will allow refinement of the thrombotic risk prediction, with a potential of enhancing the precision in the individualized antithrombotic management of a patient. This work supports further examination of the components of this thrombosis axis to stratify patients at risk for thrombosis. Although this study focused on patients with CKD, exploration of the solute-AHR-TF axis is warranted in other models of thrombosis such as venous thromboembolism and in various disorders characterized by hyperthrombotic phenotype.

CONCISE METHODS

Acquisition of sera samples, assessment of the stability and preanalytic variability of metabolites and assays, cell lines used, and selection of optimum concentrations of sera in different assays are described in the supplemental information, *i.e.*, in the legends to Supplemental Figures 5, 6, and 7, and in the Supplemental Methods.

Pattern Recognition

We leveraged both linear and nonlinear dimensionality reduction techniques to visualize high-dimensional data obtained from metabolomics and activity assays by projecting them onto a two-dimensional map while preserving the separation between “event” and “no-event” subgroups. This type of mapping takes advantage of the inherent structure of the high-dimensional data and attempts to embed the data into a subspace of lower dimensionality (typically 2D or three dimensional (3D) representations), making it convenient for one to visualize possible clustering of the subgroup data. Four different techniques were used—PCA, neighborhood components analysis, t-distributed stochastic neighbor

embedding, and locality preserving projections. These techniques are described in more detail elsewhere.^{24–26}

Generation of a Kyn-Specific Thrombosis Model

A group of C57BL/6 mice (Jackson Labs), 12–16-week-old females and males, were administered Kyn dissolved in DMSO and further diluted in PBS at 0.5 mg/kg intraperitoneally once a day, and the excretion was inhibited by probenecid (150 mg/kg administered intraperitoneally twice a day). Probenecid is an inhibitor of organic anion transporter 1 and 3, and suppresses the excretion of Kyn. Serum Kyn levels were measured on days 0 and 5, using LC/MS developed and validated for the measurement of Kyn in serum, after which the animals were subjected to FeCl₃-mediated carotid injury, performed as we described previously.³³ Briefly, the right carotid artery was exposed in animals under isoflurane anesthesia, and basal blood flow recorded using a 0.5PSB S-series flow probe connected to a TS420 perivascular transit-time flow meter (Transonic, Ithaca, NY). The probe was removed, and a piece of Whatman filter paper (1×10 mm) soaked in FeCl₃ (Sigma-Aldrich, St. Louis, MO) was placed under the carotid artery for 1 minute. After washing with warm physiologic saline (0.9% NaCl), the probe was returned, and volume of blood flow was monitored for 20 minutes starting from the placement of the filter paper. Mean, maximum, and minimum carotid flow was recorded using Powerlab Chart5 version 5.3 software, in 1-second intervals. TtO was determined as the first measurement, 0.299 ml/min. Average basal flow volume corresponds to an average of measurements over the 30 seconds preceding placement of the filter paper.

ACKNOWLEDGMENTS

The authors acknowledge Dr. David Salant (Boston University School of Medicine [BUSM]) for his valuable insights on this project and Dr. Nigel Mackman (University of North Carolina, Chapel Hill) for tissue factor activity assay. We acknowledge Dr. Nader Rahimi (BUSM) for providing Human umbilical vein endothelial cells (HUVEC)-telomerase reverse transcriptase (tert)-tert cell lines and Dr. David Sherr (BUSM) for establishing the aryl hydrocarbon receptor activity assay. We also thank the Metabolomics Core facilities of the Department of Medicine at Boston University School of Medicine.

This work was funded in part by R01HL132325, R01 CA175382, and the Evans Faculty Merit award to V.C.C.; the Hariri Research Award (#2016-10-009) from the Hariri Institute of Computing, Boston University, and the American Heart Association's Scientist Development Grant (#17SDG33670323) to V.B.K.; National Heart, Lung, and Blood Institute R01 HL080442 to K. Ravid; the Sharon Anderson Research Fellowship grant award from the American Society of Nephrology and T32 training in renal biology T32DK007053-44 to K. Rijal; and T32 training grant in cardiovascular biology T32HL007224-40 to J.W. This work was also funded in part by the Affinity Research Collaborative on the Thrombosis and Hemostasis program from the Department of Medicine at Boston University School of Medicine.

V.B.K., M.E.B., J.M.F., K. Ravid, and V.C.C. conceptualized the idea and designed the study; M.S. and K. Rijal performed the tissue factor activity assay with Thrombolysis in Myocardial Infarction (TIMI)–II

and Dialysis Access Consortium (DAC-Fistula) trial samples, respectively; F.A. and S.S. performed the aryl hydrocarbon receptor activity assay of TIMI-II and DAC trials, respectively; C.M.G. and L.M.D. provided insights into the TIMI-II and DAC-fistula studies, respectively, and assisted in data interpretation; V.B.K. and V.C.C. wrote the manuscript; M.E.B., C.M.G., L.M.D., J.M.F., and K. Ravid reviewed, edited, and contributed conceptually to the manuscript's content; V.B.K. performed the analysis; M.E.B., F.A., M.S., and S.M. performed animal model and thrombosis assays.

DISCLOSURES

None.

REFERENCES

- Mackman N: Triggers, targets and treatments for thrombosis. *Nature* 451: 914–918, 2008
- Ocak G, van Stralen KJ, Rosendaal FR, Verduijn M, Ravani P, Palsson R, et al: Mortality due to pulmonary embolism, myocardial infarction, and stroke among incident dialysis patients. *J Thromb Haemost* 10: 2484–2493, 2012
- Foley RN, Murray AM, Li S, Herzog CA, McBean AM, Eggers PW, et al: Chronic kidney disease and the risk for cardiovascular disease, renal replacement, and death in the United States Medicare population, 1998 to 1999. *J Am Soc Nephrol* 16: 489–495, 2005
- Iakovou I, Schmidt T, Bonizzi E, Ge L, Sangiorgi GM, Stankovic G, et al: Incidence, predictors, and outcome of thrombosis after successful implantation of drug-eluting stents. *JAMA* 293: 2126–2130, 2005
- Chillon JM, Massy ZA, Stengel B: Neurological complications in chronic kidney disease patients. *Nephrol Dial Transplant* 31: 1606–1614, 2016
- Garimella PS, Hart PD, O'Hare A, DeLoach S, Herzog CA, Hirsch AT: Peripheral artery disease and CKD: A focus on peripheral artery disease as a critical component of CKD care. *Am J Kidney Dis* 60: 641–654, 2012
- Kimura T, Morimoto T, Kozuma K, Honda Y, Kume T, Aizawa T, et al; RESTART Investigators: Comparisons of baseline demographics, clinical presentation, and long-term outcome among patients with early, late, and very late stent thrombosis of sirolimus-eluting stents: Observations from the Registry of Stent Thrombosis for Review and Reevaluation (RESTART). *Circulation* 122: 52–61, 2010
- Cassler LF, Dember LM: Thrombosis in end-stage renal disease. *Semin Dial* 16: 245–256, 2003
- Shashar M, Belghasem ME, Matsuura S, Walker J, Richards S, Alousi F, et al: Targeting STUB1-tissue factor axis normalizes hyperthrombotic uremic phenotype without increasing bleeding risk. *Sci Transl Med* 9, 2017
- Chitalia VC, Shivanna S, Martorell J, Balcells M, Bosch I, Kolandaivelu K, et al: Uremic serum and solutes increase post-vascular interventional thrombotic risk through altered stability of smooth muscle cell tissue factor. *Circulation* 127: 365–376, 2013
- Shivanna S, Kolandaivelu K, Shashar M, Belghasim M, Al-Rabadi L, Balcells M, et al: The aryl hydrocarbon receptor is a critical regulator of tissue factor stability and an antithrombotic target in uremia. *J Am Soc Nephrol* 27: 189–201, 2016
- Yang K, Du C, Wang X, Li F, Xu Y, Wang S, et al: Indoxyl sulfate induces platelet hyperactivity and contributes to chronic kidney disease-associated thrombosis in mice. *Blood* 129: 2667–2679, 2017
- Gondouin B, Cerini C, Dou L, Sallée M, Duval-Sabatier A, Pletinck A, et al: Indolic uremic solutes increase tissue factor production in endothelial cells by the aryl hydrocarbon receptor pathway. *Kidney Int* 84: 733–744, 2013

14. Dember LM, Beck GJ, Allon M, Delmez JA, Dixon BS, Greenberg A, et al; Dialysis Access Consortium Study Group: Effect of clopidogrel on early failure of arteriovenous fistulas for hemodialysis: A randomized controlled trial. *JAMA* 299: 2164–2171, 2008
15. Braunwald E: Thrombolysis in myocardial infarction (TIMI) phase II trial. *N Engl J Med* 321: 612, 1989
16. Roy-Chaudhury P, Sukhatme VP, Cheung AK: Hemodialysis vascular access dysfunction: A cellular and molecular viewpoint. *J Am Soc Nephrol* 17: 1112–1127, 2006
17. Harnek J, Zoucas E, Carlemalm E, Cwikiel W: Differences in endothelial injury after balloon angioplasty, insertion of balloon-expanded stents or release of self-expanding stents: An electron microscopic experimental study. *Cardiovasc Intervent Radiol* 22: 56–61, 1999
18. Srikanth S, Ambrose JA: Pathophysiology of coronary thrombus formation and adverse consequences of thrombus during PCI. *Curr Cardiol Rev* 8: 168–176, 2012
19. Zhang A, Rijal K, Ng SK, Ravid K, Chitalia V: A mass spectrometric method for quantification of tryptophan-derived uremic solutes in human serum. *J Biol Methods* 4: 75, 2017
20. Dember LM, Kaufman JS, Beck GJ, Dixon BS, Gassman JJ, Greene T, et al; DAC Study Group: Design of the Dialysis Access Consortium (DAC) clopidogrel prevention of early AV fistula thrombosis trial. *Clin Trials* 2: 413–422, 2005
21. Eddy DM, Hollingworth W, Caro JJ, Tsevat J, McDonald KM, Wong JB; ISPOR-SMDM Modeling Good Research Practices Task Force: Model transparency and validation: A report of the ISPOR-SMDM Modeling Good Research Practices Task Force-7. *Med Decis Making* 32: 733–743, 2012
22. Pawlak K, Mysliwiec M, Pawlak D: Hypercoagulability is independently associated with kynurenine pathway activation in dialysed uraemic patients. *Thromb Haemost* 102: 49–55, 2009
23. Vanholder R, Glorieux G: Introduction: Uremic toxicity - state of the art 2014. *Semin Nephrol* 34: 85–86, 2014
24. Tenenbaum JB, de Silva V, Langford JC: A global geometric framework for nonlinear dimensionality reduction. *Science* 290: 2319–2323, 2000
25. Roweis ST, Saul LK: Nonlinear dimensionality reduction by locally linear embedding. *Science* 290: 2323–2326, 2000
26. Pang R, Lansdell BJ, Fairhall AL: Dimensionality reduction in neuroscience. *Curr Biol* 26: R656–R660, 2016
27. Hinton GE, Salakhutdinov RR: Reducing the dimensionality of data with neural networks. *Science* 313: 504–507, 2006
28. Stejskalova L, Dvorak Z, Pavek P: Endogenous and exogenous ligands of aryl hydrocarbon receptor: Current state of art. *Curr Drug Metab* 12: 198–212, 2011
29. Kawasaki H, Chang HW, Tseng HC, Hsu SC, Yang SJ, Hung CH, et al: A tryptophan metabolite, kynurenine, promotes mast cell activation through aryl hydrocarbon receptor. *Allergy* 69: 445–452, 2014
30. Zhao B, Degroot DE, Hayashi A, He G, Denison MS: CH223191 is a ligand-selective antagonist of the Ah (Dioxin) receptor. *Toxicol Sci* 117: 393–403, 2010
31. Uwai Y, Honjo H, Iwamoto K: Interaction and transport of kynurenic acid via human organic anion transporters hOAT1 and hOAT3. *Pharmacol Res* 65: 254–260, 2012
32. Saito K, Fujigaki S, Heyes MP, Shibata K, Takemura M, Fujii H, et al: Mechanism of increases in L-kynurenine and quinolinic acid in renal insufficiency. *Am J Physiol Renal Physiol* 279: F565–F572, 2000
33. Matsuura S, Mi R, Koupenova M, Eliades A, Patterson S, Toselli P, et al: Lysyl oxidase is associated with increased thrombosis and platelet reactivity. *Blood* 127: 1493–1501, 2016
34. Cheng S, Larson MG, McCabe EL, Murabito JM, Rhee EP, Ho JE, et al: Distinct metabolomic signatures are associated with longevity in humans. *Nat Commun* 6: 6791, 2015
35. Lim CK, Bilgin A, Lovejoy DB, Tan V, Bustamante S, Taylor BV, et al: Kynurenine pathway metabolomics predicts and provides mechanistic insight into multiple sclerosis progression. *Sci Rep* 7: 41473, 2017
36. Wu CC, Hsieh MY, Hung SC, Kuo KL, Tsai TH, Lai CL, et al: Serum indoxyl sulfate associates with postangioplasty thrombosis of dialysis grafts. *J Am Soc Nephrol* 27: 1254–1264, 2016
37. Zuo H, Ueland PM, Ulvik A, Eussen SJ, Vollset SE, Nygård O, et al: Plasma biomarkers of inflammation, the kynurenine pathway, and risks of all-cause, cancer, and cardiovascular disease mortality: The Hordaland Health study. *Am J Epidemiol* 183: 249–258, 2016
38. Pedersen ER, Tuseth N, Eussen SJ, Ueland PM, Strand E, Svingen GF, et al: Associations of plasma kynurenines with risk of acute myocardial infarction in patients with stable angina pectoris. *Arterioscler Thromb Vasc Biol* 35: 455–462, 2015
39. Pawlak K, Tankiewicz J, Mysliwiec M, Pawlak D: Tissue factor/its pathway inhibitor system and kynurenines in chronic kidney disease patients on conservative treatment. *Blood Coagul Fibrinolysis* 20: 590–594, 2009
40. Wu D, Nishimura N, Kuo V, Fiehn O, Shahbaz S, Van Winkle L, et al: Activation of aryl hydrocarbon receptor induces vascular inflammation and promotes atherosclerosis in apolipoprotein E-/- mice. *Arterioscler Thromb Vasc Biol* 31: 1260–1267, 2011
41. Sherr DH: Another important biological function for the aryl hydrocarbon receptor. *Arterioscler Thromb Vasc Biol* 31: 1247–1248, 2011
42. Steffel J, Lüscher TF, Tanner FC: Tissue factor in cardiovascular diseases: Molecular mechanisms and clinical implications. *Circulation* 113: 722–731, 2006
43. Lippi G, Franchini M: Pathogenesis of venous thromboembolism: When the cup runneth over. *Semin Thromb Hemost* 34: 747–761, 2008
44. Kumar G, Sakhuja A, Taneja A, Majumdar T, Patel J, Whittle J, et al; Milwaukee Initiative in Critical Care Outcomes Research (MICCOR) Group of Investigators: Pulmonary embolism in patients with CKD and ESRD. *Clin J Am Soc Nephrol* 7: 1584–1590, 2012
45. Shashar M, Francis J, Chitalia V: Thrombosis in the uremic milieu—emerging role of “thrombolome”. *Semin Dial* 28: 198–205, 2015
46. Kolodziej LR, Paleolog EM, Williams RO: Kynurenine metabolism in health and disease. *Amino Acids* 41: 1173–1183, 2011
47. Kennedy PJ, Cryan JF, Dinan TG, Clarke G: Kynurenine pathway metabolism and the microbiota-gut-brain axis. *Neuropharmacology* 112 [Pt B]: 399–412, 2017
48. Schefold JC, Zeden JP, Fotopoulou C, von Haehling S, Pschowski R, Hasper D, et al: Increased indoleamine 2,3-dioxygenase (IDO) activity and elevated serum levels of tryptophan catabolites in patients with chronic kidney disease: A possible link between chronic inflammation and uraemic symptoms. *Nephrol Dial Transplant* 24: 1901–1908, 2009
49. Cheung AK, Imrey PB, Alpers CE, Robbin ML, Radeva M, Larive B, et al; Hemodialysis Fistula Maturation Study Group: Intimal hyperplasia, stenosis, and arteriovenous fistula maturation failure in the hemodialysis fistula maturation study. *J Am Soc Nephrol* 28: 3005–3013, 2017
50. Liabeuf S, Drüeke TB, Massy ZA: Protein-bound uremic toxins: New insight from clinical studies. *Toxins (Basel)* 3: 911–919, 2011
51. Barreto FC, Barreto DV, Liabeuf S, Meert N, Glorieux G, Temmar M, et al; European Uremic Toxin Work Group (EUTox): Serum indoxyl sulfate is associated with vascular disease and mortality in chronic kidney disease patients. *Clin J Am Soc Nephrol* 4: 1551–1558, 2009
52. Miller WG, Myers GL, Ashwood ER, Killeen AA, Wang E, Thienpont LM, et al: Creatinine measurement: State of the art in accuracy and inter-laboratory harmonization. *Arch Pathol Lab Med* 129: 297–304, 2005

This article contains supplemental material online at <http://jasn.asnjournals.org/lookup/suppl/doi:10.1681/ASN.2017080929/-/DCSupplemental>.

Supplementary methods:

Sera processing and analysis of metabolites:

We acquired sera from two previous NIH-funded clinical trials to probe for the uremic solute-AHR-TF axis after an Institutional Review Board approval. DAC and TIMI-II trial cohorts served as appropriate datasets, given thrombotic events in the patients undergoing vascular interventions such as fistula surgery or balloon angioplasty, respectively, and the availability of serum samples. The samples were thawed once, aliquoted in smaller volume for different assays and snap frozen immediately and were stored in a dedicated -80 freezer. The sera samples were subjected to a targeted metabolomics analysis using methods previously described^{11, 19}. NHLBI deems a sample 'low impact' if the serum is available in sufficient quantity and will not get depleted to more than 50% of the current amount after sharing for a proposed study. We acquired 377 'low impact' sera samples from TIMI-II trial and 473 samples from DAC-fistula trial for this study.

Stability of the solutes and functional assays:

This study examined human sera samples from two clinical trials that were performed several years ago (DAC in 2003-2007 and TIMI-II in 1986-1988). As these samples were frozen and stored at -80°C, we examined the effect of storage on the stability of the metabolites and AHR and TF activity levels. Specifically, the levels of metabolites, AHR and TF activities in the same set of sera samples were analyzed twice over four years of storage (2012-2016). Ten patients with end stage renal disease (ESRD) treated at Boston University Medical Center were selected from a group described previously^{9, 11}. This group consisted of ten African American ESRD patients predominantly males (N = 8) with median age 42 years (range 31-53 years). While testing the effect of the entire storage period of

these two clinical trials was not feasible, our results showed no significant effect of four years of storage on the levels of the metabolites and AHR or TF activities (**Supplementary Figure 5A-5C**).

Cell lines:

Primary human aortic vSMCs obtained from ATCC were grown in DMEM low glucose with 5% calf serum and 1% penicillin and streptomycin and used up to 10 passages. HepG3 cells and HUVEC-tert cells were grown DMEM with high glucose and 5% calf serum and 1% penicillin and streptomycin.

For TF activity, we used both primary human aortic vascular smooth muscle cells (vSMCs) and endothelial cells. For the DAC-fistula study, TF activity was also analyzed in the immortalized human umbilical endothelial cells (HUVEC-tert). While we considered the option of using primary human umbilical endothelial cells (Lonza, USA), we observed a batch-to-batch variation in response to TF activity. For example, a set of sera samples elicited TF activity in three independent batches of HUVECs with coefficient of variation (CV) by 38.5%, suggesting their unsuitability to be used for such study. Therefore, we immortalized HUVECs and after performing both a biochemical characterizing of the cell line using endothelial cell-specific markers and functional characterization with an in vitro angiogenesis assay for up to 15 passages, we used for TF activity assay. This provided us with sufficient number of passages to allow screening of 870 samples with minimal variability (CV 13-18%) of TF activity over 6-8 passages). These immortalized HUVECs called HUVEC-tert cells, which were generated by transducing the primary pooled human umbilical vein endothelial cells (HUVECs, Lonza, USA) with a retrovirus expressing telomerase.

The persistence of endothelial characteristics over 15 passages was confirmed by different ways as described below. The lysates from these cells were probed for vascular endothelial cadherin (VE cadherin), which still persisted in HUVEC-tert similar to HUVECs, but not in NIH 3T3 fibroblast cells and HK-2 cells (human kidney epithelial cells) (**Supplementary Figure 6A**). Functional evaluation of these cells was performed using *in-vitro* angiogenesis or tube formation assay (**Supplementary Figures 6B and 6C**). 15,000 HUVEC-tert cells were seeded in 96-well plates precoated with 100 μ l of growth factor-poor Matrigel™ (BD Biosciences) (10 mg/ml) and incubated at 37°C for 24 hours. Tube formation was imaged using phase contrast microscopy and tube lengths were analyzed using ImageJ software. The tube formation with HUVEC and HUVEC-tert samples was similar. No tube formation was observed with fibroblast or epithelial cells. These data confirm the persistence of the endothelial phenotype in HUVEC-tert cells up to 15 passages. TF activity was examined within 10 passages of these cells.

AHR activity:

AHR Activity was measured in HUEC-tert, as described previously (**Supplementary Figure 1A**)¹¹. Briefly, the cell lines stably expressing a Cignal Lenti Reporter xenobiotic response element tethered to luciferase reporter (XRE-luc) (Qiagen, CLS-9045L-8) were used. The cells seeded at 1000/well in 96-well plate were serum starved for 16 hours and then treated with the serum with or without AHR inhibitor, CH223191 for 24 hours. Firefly luciferase activity was measured using luciferase assay kit (Promega# E1501). After luciferase assay, the cells were lysed in RIPA buffer and the protein content was

determined using Bradford assay. The luciferase signal was then normalized to protein content (relative luciferase activity unit).

TF procoagulant activity:

TF surface or surface procoagulant activity was measured using a two-step FXa generation assay, as described previously¹¹ (**Supplementary Figure 1B**). A standard curve was generated by incubating human recombinant lipidated TF (Enzo lifesciences, Cat# SE-537) ranging from 0-500 pM along with 5 nM of human factor VIIa (Enzyme Research Laboratories Cat# HFVIIa) and 150 nM of factor X (Enzyme Research Laboratories Cat# HFX 1010) and CaCl₂- 5 mM for 30 minutes at 37°C. The reaction mixture was incubated with chromogenic substrate for factor Xa (Chromogenix Cat# S2765, 1mM-final concentration). The reaction was stopped after 5 minutes using 10 ul of 50% glacial acetic acid and read at 405 nm absorbance.

In vSMCs, the TF procoagulant activity was examined in a 96 well plate format with 1000 vSMCs seeded per well. The cells were serum starved for 16 hours and treated with 1% sera for 24 hours. Cells were washed with Tris Buffer Saline (TBS) (50 mM Tris HCl, 120 mM NaCl, 2.7 mM KCl, 3mg/ml BSA, pH=7.4) and incubated with 55 ul TBS containing 5 nM of human factor VIIa and 150 nM of factor X and CaCl₂- 5mM for 30 minutes at 37°C. 50 ul of the supernatant was incubated with chromogenic substrate at 1 mM-final concentration. The reaction was stopped after 5 minutes by adding 10 ul of 50% glacial acetic acid and the absorbance was read at 405 nm. TF activity levels in samples were calculated using regression analysis. To confirm the specificity of the TF activity assay, activity was measured in cells pre-treated with anti-TF neutralizing antibody (50 ug/ml)

(1H10) or control antibody for an hour, as described previously¹¹. TF activity was normalized to the number of cells.

The number of viable cells was determined using Alamar Blue assay (ThermoFisher Scientific). To create the standard curve, serial dilution of VSMCs cells was performed in a black, clear-bottom 96 well plate. Cells were then treated with Alamar Blue for one hour. After one hour, the fluorescence intensity of Alamar Blue was measured at 570 nm using Infinite microplate reader from Tecan. The fluorescence readout using Alamar Blue is linear over a range of ~500 to 50,000 cells per manufacturer insert. By serial dilution of cells, we obtained a linear standard curve with $R^2 = 0.97$ (**Supplementary Figure 6D**). For normalization of TF activity, after TF activity measurement, the cells were washed with 1X PBS and 100 μ l of media was added and incubated with Alamar Blue for one hour at 37 °C in CO₂ incubator. The fluorescence was measured at 750 nm and standard curve was applied to obtain the number of viable cells.

Determining the optimum concentrations of the sera used for the DAC and TIMI-II studies:

Before examining the samples for AHR and TF activity assays, we determined the optimal concentration of serum for the DAC and TIMI-II trials to be used for these assays. A titrated concentration of sera from five randomly selected subjects from the DAC trial was used on HepG2 and vSMCs for AHR and TF activities, respectively. The specificity of both AHR and TF activation was further confirmed by co-treating the sample with a competitive AHR inhibitor – CH223191³⁰, which has been previously shown to inhibit both the AHR and TF activities¹¹. Our results showed that one percent and five percent of sera resulted in the highest level of AHR and TF activities, respectively, and were suppressed by 70-80% with

CH223191 (**Supplementary Figures 7A-7B**). A similar analysis was performed in TIMI-II samples (**Supplementary Figures 7C and 7D**). One percent of serum resulted in the highest level of both AHR and TF activities, respectively, which were suppressed with CH223191. Based on these results, for DAC study, we used 1% serum for AHR Activity and 5% serum for TF activity assay, while 1% serum was used for both the assays in TIMI-II study.

Cell lysis and Western blotting:

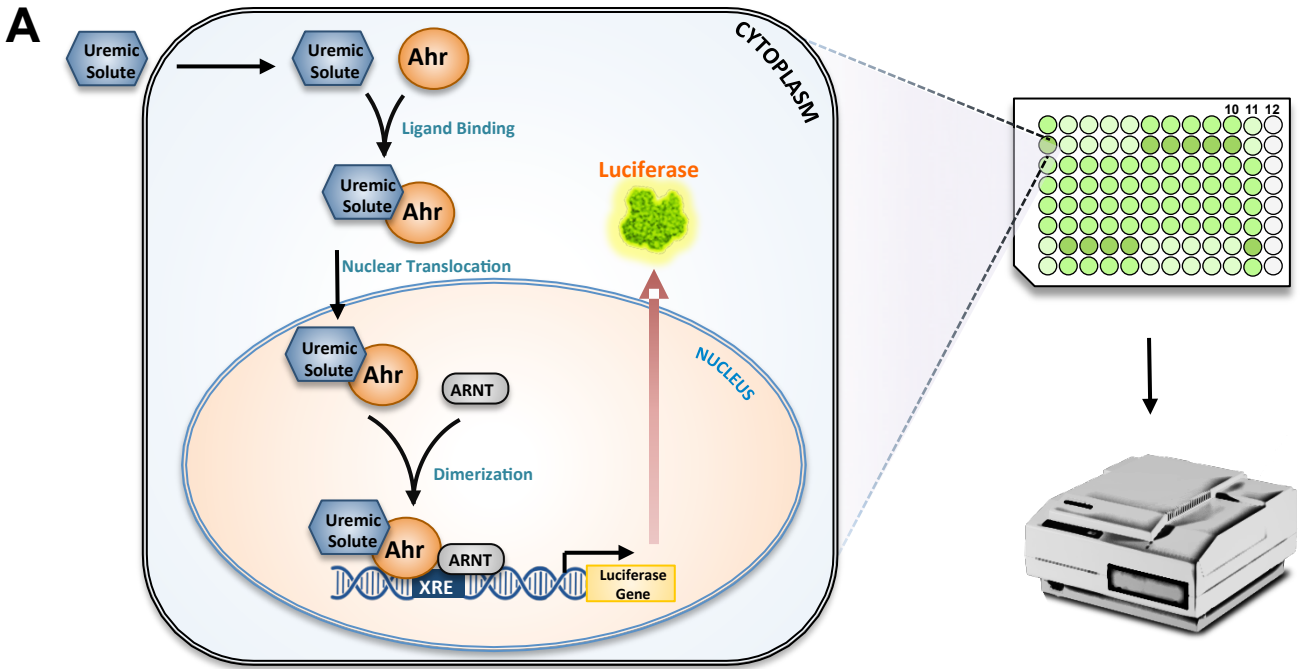
Cell harvest and immunoblotting have been described previously⁹. Monoclonal antibodies specific for tissue factor (Thermoscientific), GAPDH (Cell signaling) 1:1000 dilutions were used. CH223191 was purchased from Sigma (Catalogue C8124) and was dissolved in DMSO.

Institutional approval:

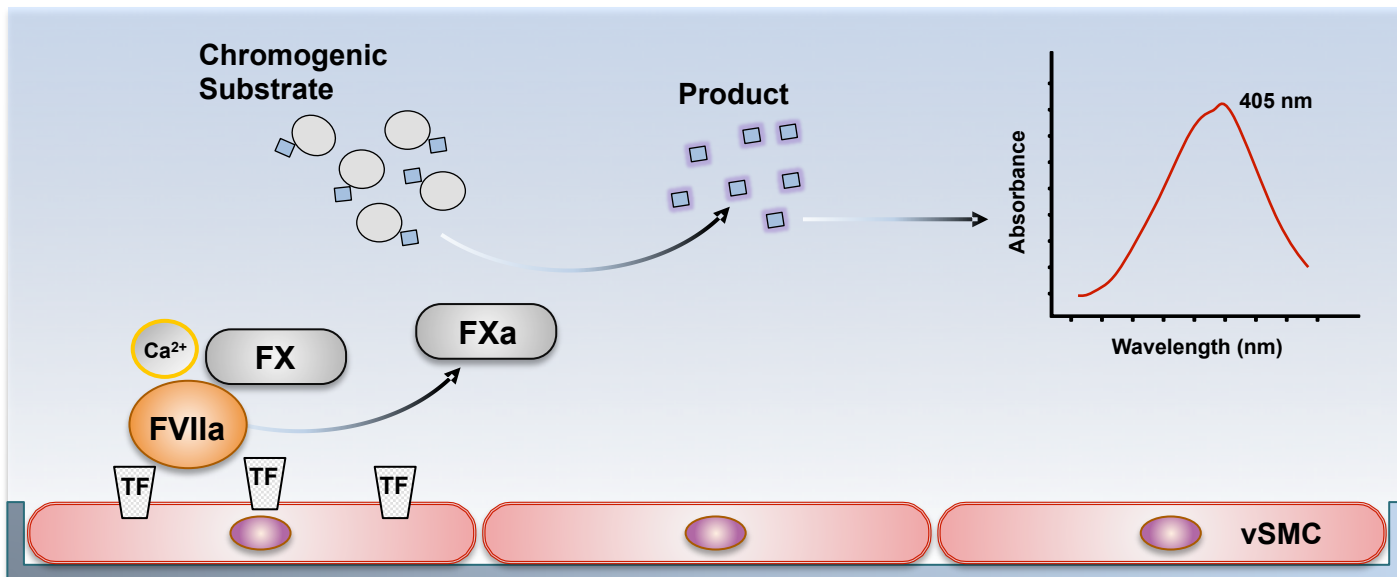
All experiments were performed under IRB protocol H-32525, reviewed and approved by Boston University. Animal studies were approved by IACUC protocol # A.N15449.

Statistical analysis:

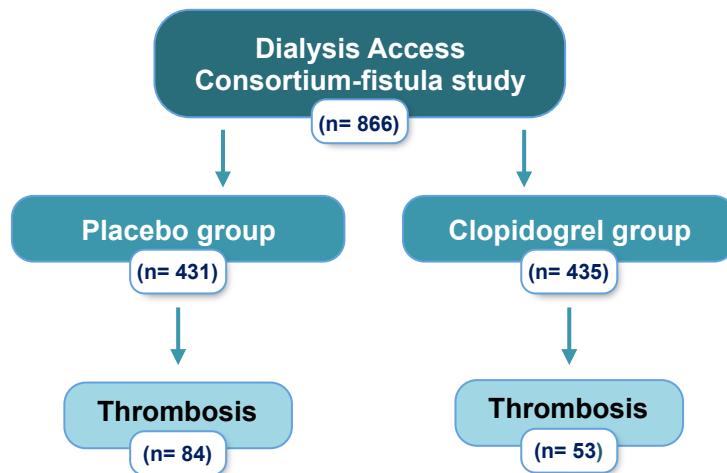
Summary statistics are presented as the mean, median and SD. Either a Student's t-test or Fisher's exact test was performed to compare the groups as appropriate. Spearman or Pearson correlation was performed to analyze correlation between two variables, as appropriate. Statistical significance was assessed at $p < 0.05$.



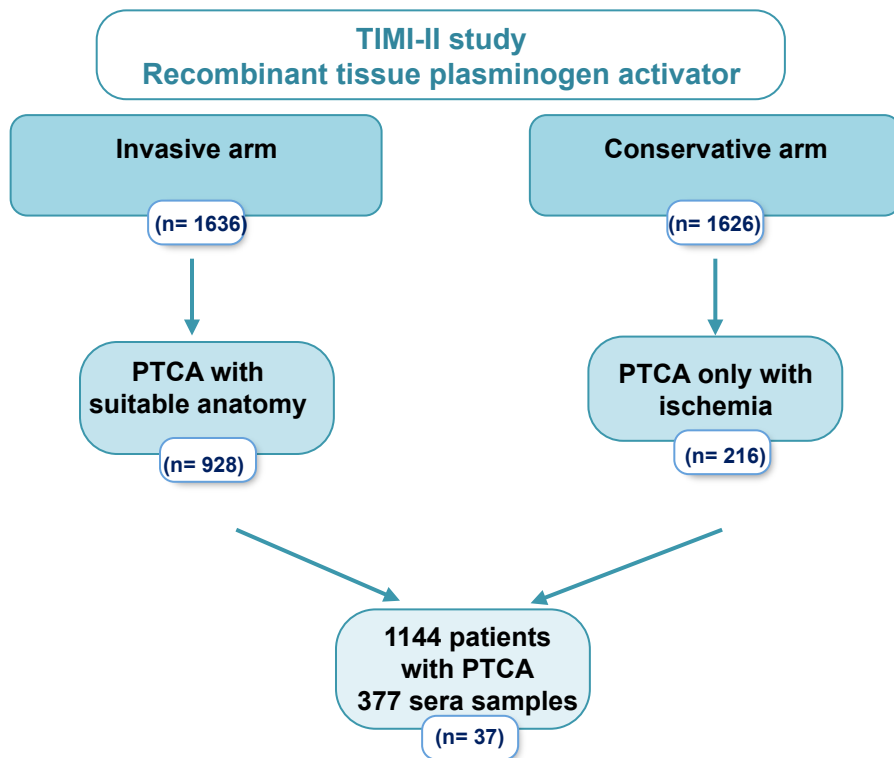
B



C



D



Supplementary Figure 1. Trial design

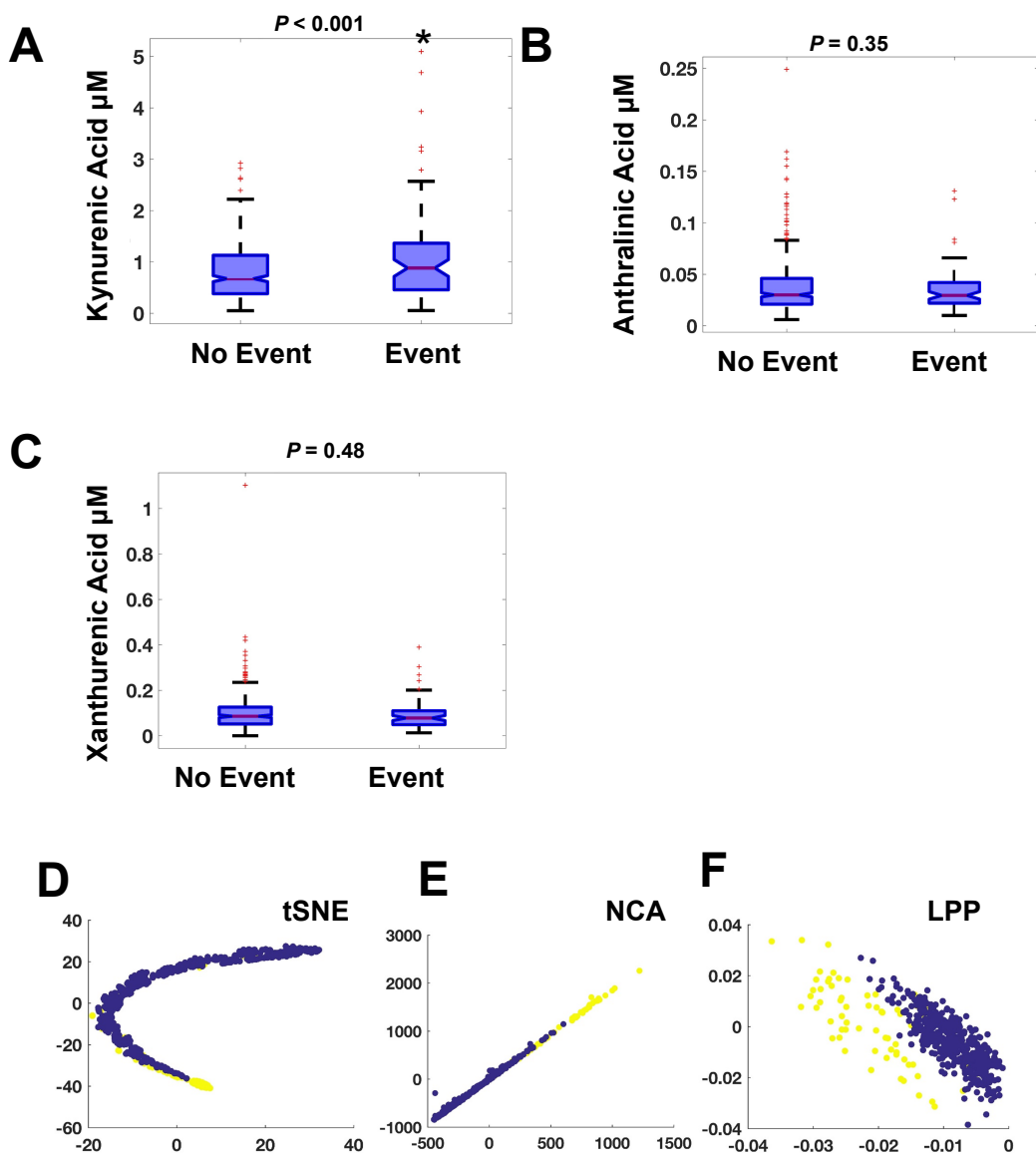
(A). AHR activity assay: AHR activity was examined in HUVEC-tert cells stably expressing Cignal Lenti Reporter xenobiotic response element tethered to luciferase reporter gene (XRE-luc). Cells seeded at 1000/well in a 96-well plate were serum starved for 16 hours and treated with a pre-defined serum concentration. The firefly luciferase measured using luciferase assay was normalized to protein concentration.

(B). TF activity assay: TF surface/procoagulant activity was measured using a two-step FXa generation assay in a 96 well plate format seeded with primary human aortic vascular smooth muscle cells (vSMCs) or human umbilical vein endothelial cells. The cells were treated with pre-defined serum concentration, followed by incubation with human factor VIIa and factor X and CaCl₂. The TF converts Factor X to Xa, which is measured using a chromogenic substrate that changes color measured at 405 nm. A standard curve generated using recombinant TF provides the amount of TF activity and normalized to 10³ cells.

(C). DAC was a randomized, double-blind, placebo-controlled trial conducted from 2003-2007 with 877 participants with end stage renal disease (ESRD) or advanced chronic kidney disease who underwent surgical creation of an arteriovenous fistula for hemodialysis. Participants were randomly assigned to receive clopidogrel (n = 441) or placebo (n = 436) for 6 weeks starting within 1 day after fistula creation. The primary outcome was fistula thrombosis, determined by physical examination at 6 weeks. The secondary outcome was failure of the fistula to become suitable for dialysis defined as use of the fistula at a dialysis machine blood pump rate of 300 mL/min or more during 8 of 12 dialysis sessions during the 5th month after fistula creation. Fistula thrombosis occurred in

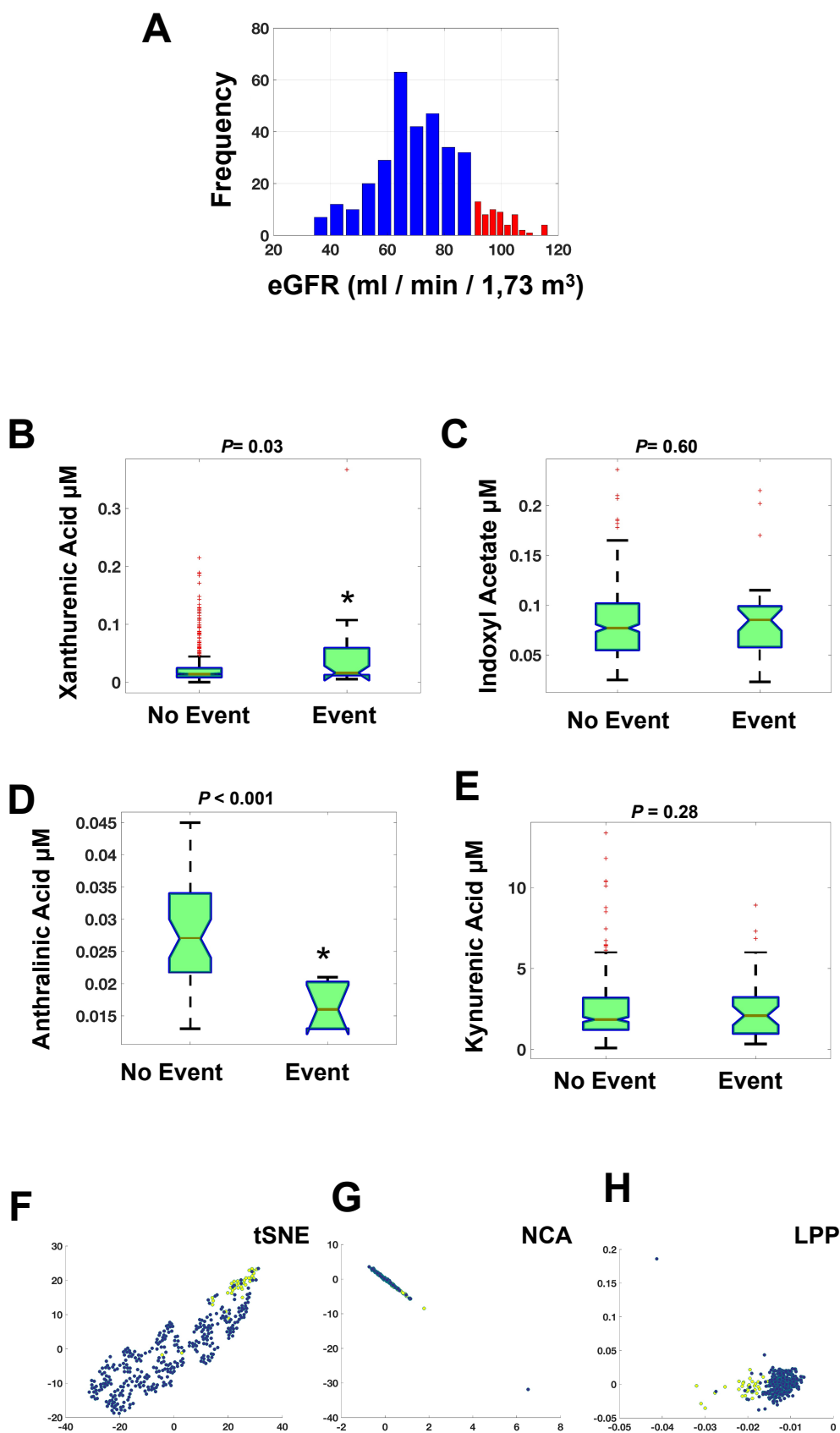
53 (12.2%) participants assigned to clopidogrel compared with 84 (19.5%) participants assigned to placebo. Failure to attain suitability for dialysis did not differ between the clopidogrel and placebo groups (61.8% vs 59.5%, respectively).

(D). TIMI-II was a randomized interventional multicenter trial conducted from 1993-1998 with 3262 participants who were treated with intravenous recombinant plasminogen activator within four hours of onset of chest pain with ST elevation myocardial infarction. Of the total participants, 1636 were randomized to receive coronary angiography within 18-48 hours of treatment of recombinant plasminogen activator followed by prophylactic percutaneous transluminal coronary angioplasty (PTCA) if arteriography demonstrated suitable anatomy (invasive arm). 1626 participants were randomized to a conservative strategy wherein patients underwent arteriography and PTCA only with spontaneous or exercise-induced ischemia. In the invasive arm, PTCA was attempted in 928 of 1636 patients. In the conservative arm, 216 patients underwent PTCA. Serum samples from 377 of 1144 patients who underwent PTCA were tested. Among the 377 participants with the baseline serum samples, 37 patients had reinfarction or reocclusion after PTCA, which were considered as 'events' for the current study.



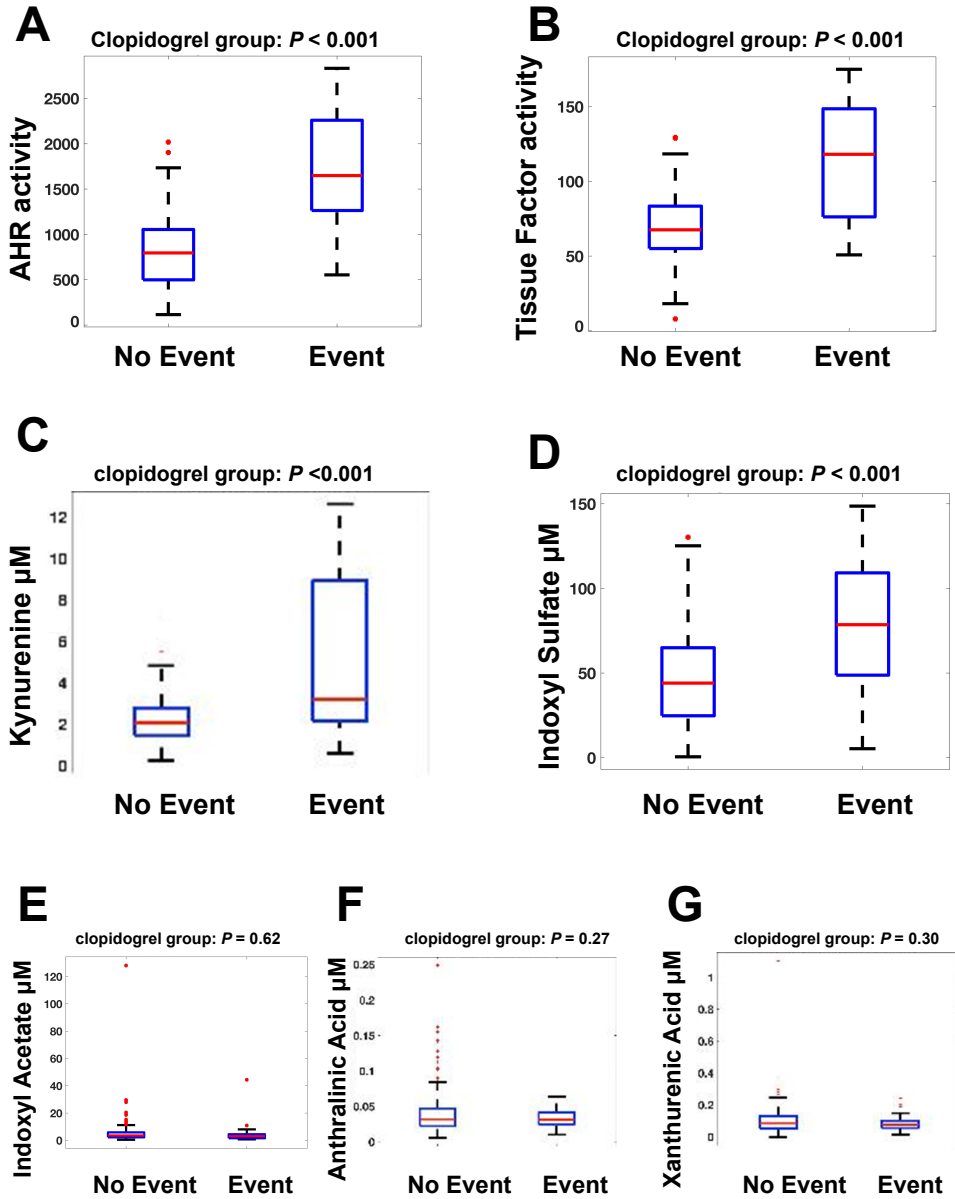
Supplementary Figure 2. Metabolites and pattern recognition algorithms in DAC-fistula trial

(A, B, C) Box plots showing the differences in the metabolites between the AVF thrombosis 'event' and 'no-event' groups. **(D, E, F)** Different dimensionality reduction techniques such as t-distributed stochastic neighbor embedding (t-SNE), neighborhood component analysis (NCA) and locality preserving projections (LPP), respectively were used to transform the metabolite-activity data into two dimensions, and represented in plots. The patients belonging to the AVF thrombosis 'event' group are shown in yellow and ones in the 'no-event' group are shown in blue.

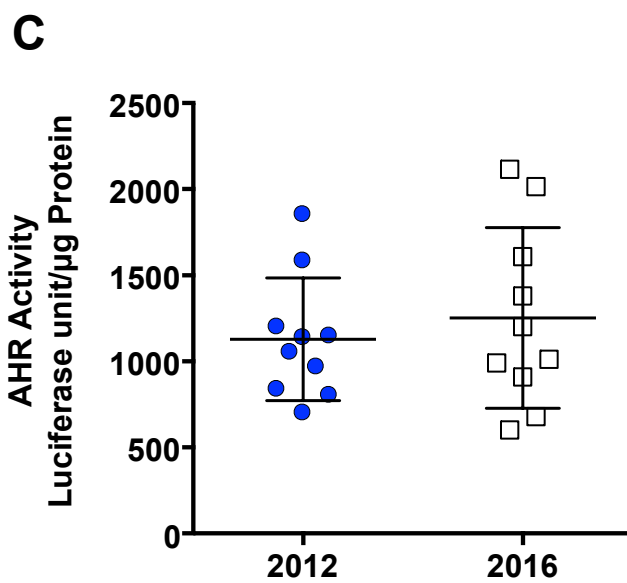
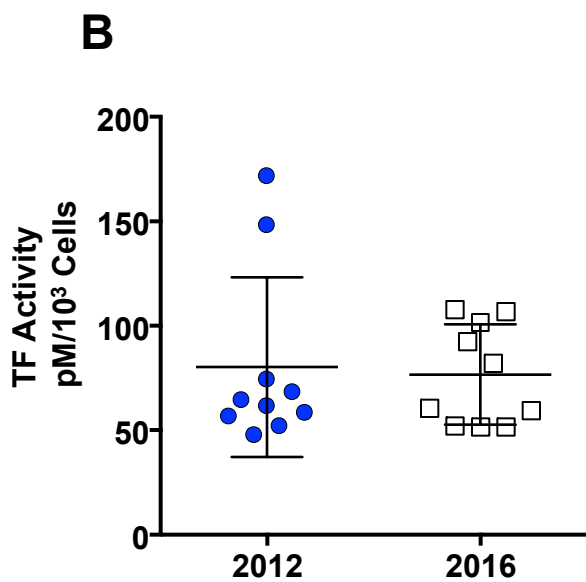
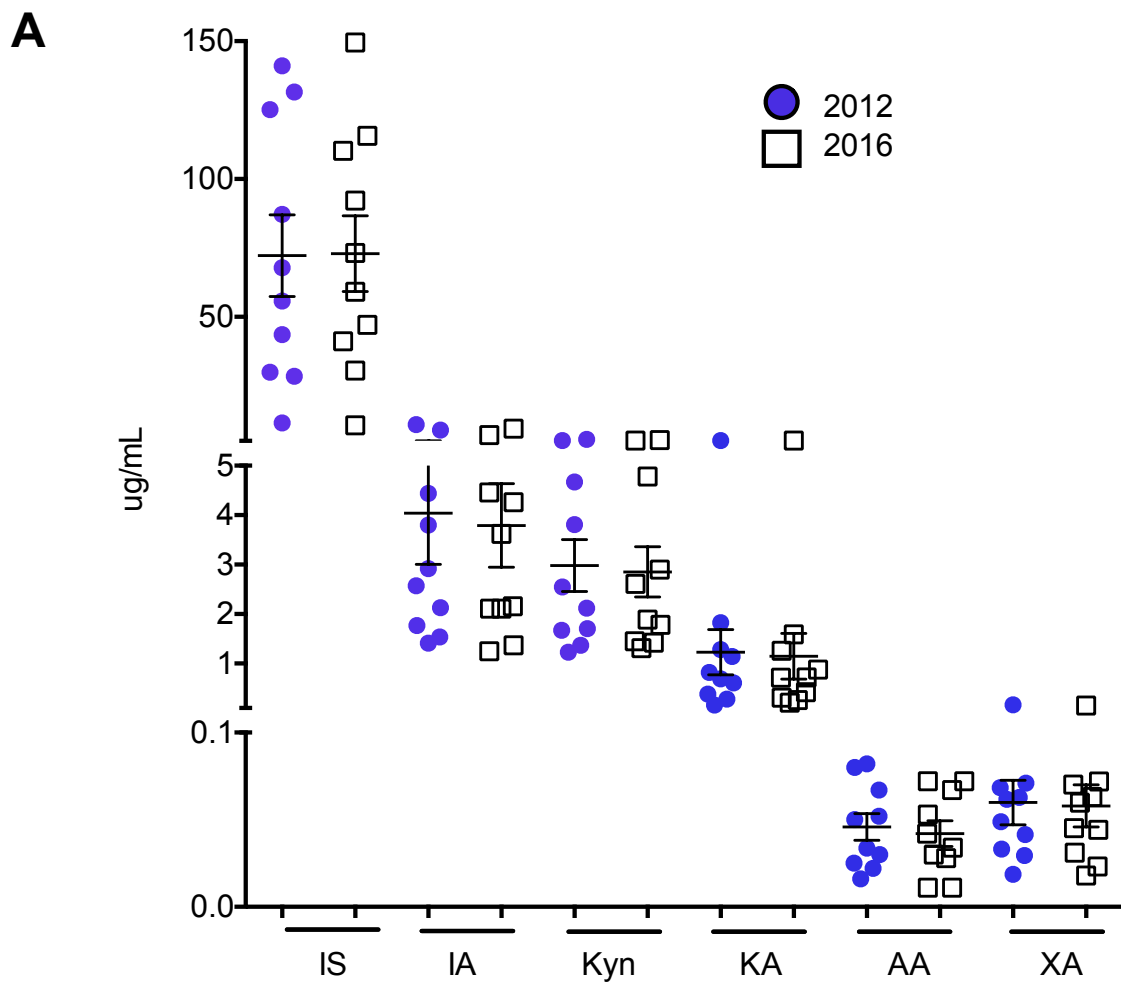


Supplementary Figure 3. Metabolites and pattern recognition algorithms in TIMI-II trial

(A) Histogram representing the eGFR distribution within the TIMI-II patient cohort. The eGFR of > 90 ml/min calculated using CKD-EPI equation was considered normal (shown in red). CKD was defined as patients with eGFR < 90 ml/min (shown in blue). **(B, C, D, E)** Box plots showing the differences of different metabolites between the 'event' and 'no-event' groups, as defined in the text for the TIMI-II trial. **(F, G, H)** Different dimensionality reduction techniques such as t-SNE, NCA, and LPP, respectively, were used to reduce the data into two dimensions, and show in a plot. The patients belonging to the 'event' group are shown in yellow and ones in the 'no-event' group are shown in blue.



Supplementary Figure 4. Activation of the thrombosis axis in the clopidogrel group. A subgroup analysis of patients who received clopidogrel in the DAC fistula study is shown. Box plots show the differences between the AVF thrombosis 'event' and 'no-event' groups for the TF and AHR activities (A and B, respectively) and individual metabolites (C-G).



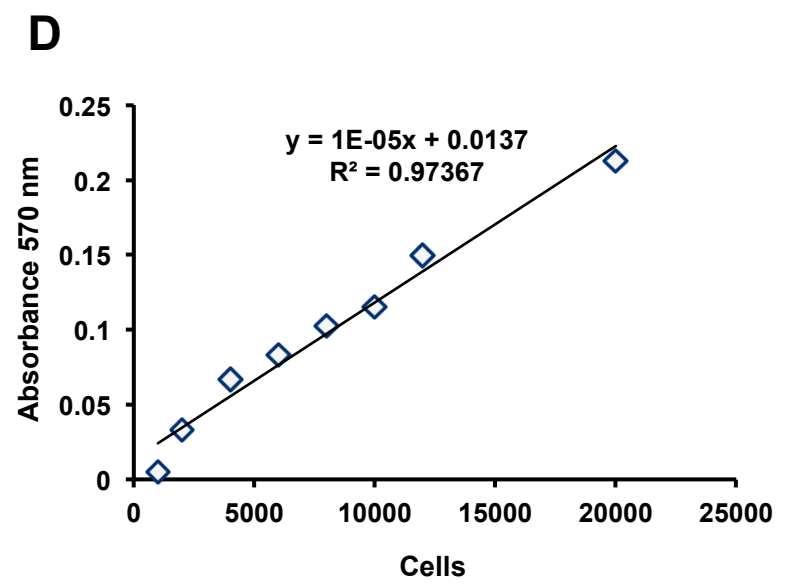
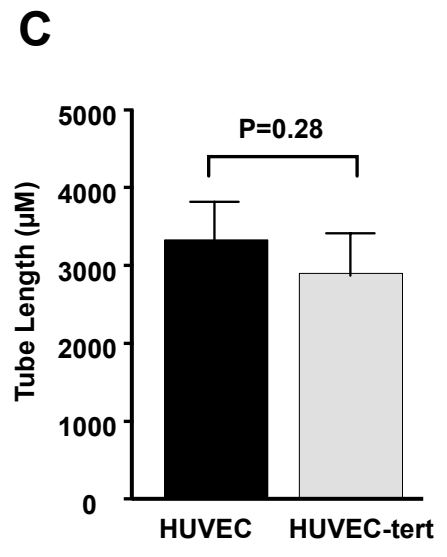
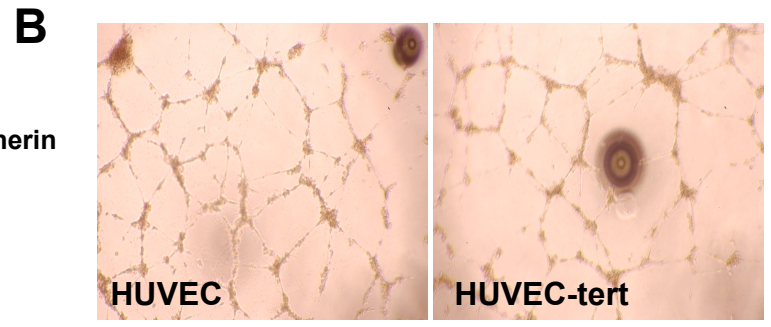
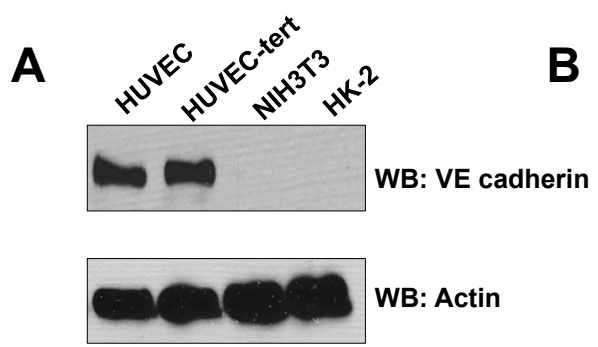
Supplementary Figure 5. Pre-analytic variability and the effect of storage of the components of thrombosis axis

(A) No effect of storage on the stability of metabolites. A set of ten sera samples from patients with end stage renal disease (ESRD) treated at Boston Medical Center was selected from a previously described group of 20 patients⁹ to test the effects of storage on stability of indoxyl sulfate (IS), indoxyl acetate (IA), kynurenine (Kyn), kynurenic acid (KA), and anthranilic acid (AA) and xanthurenic acid (XA). Serum samples frozen and stored at -80°C in two separate aliquots were examined in 2012 and 2016. There were no significant differences observed in the concentration of these uremic solutes in the samples from 2012 when compared to the same samples analyzed in 2016 (non-parametric *t*-test, $p < 0.05$). The specific *p*-values for each metabolite using a two-tailed *t*-test were 0.857 (IS), 0.459 (IA), 0.392 (Kyn), 0.403 (KA), and 0.704 (AA) and 0.362 (XA).

(B) No significant effect of four years of storage on TF Activity assay. TF activity was performed on ten samples randomly selected from a set of twenty ESRD patients as described above. The surface procoagulant TF assay was performed, as described previously on vSMCs¹¹ on the same set of sera stored in aliquots over four. There was no significant difference in TF activity in the samples from 2012 when compared to the same samples analyzed in 2016 (non-parametric *t*-test, $p < 0.05$). The specific *p*-value using a Student's *t*-test (two tailed) was 0.726.

(C) AHR activity did not differ in samples stored over four years period. AHR activity was performed in the same aliquots of sera stored over four year period, as described previously¹¹. There was no significant difference in AHR activity in the samples from 2012

when compared to the same samples analyzed in 2016 (non-paramedic t -test, $p < 0.05$). The specific p -value using a two-tailed t -test was 0.273.



Supplementary Figure 6. Persistent endothelial features in HUVEC-tert cells after 15 passages.

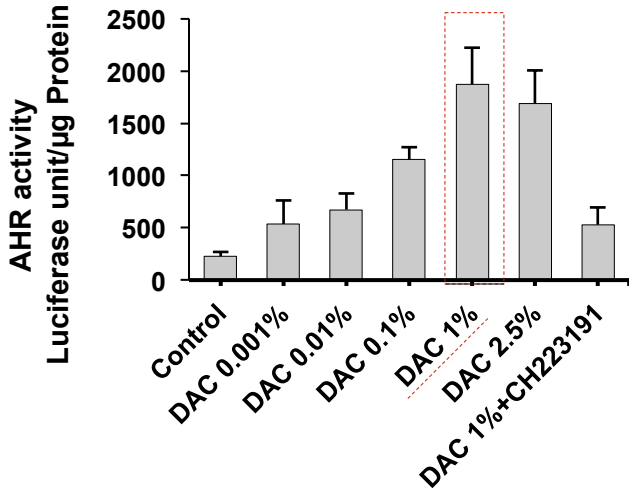
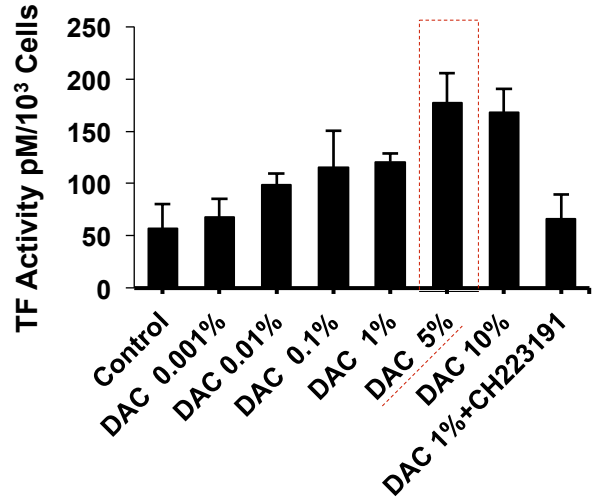
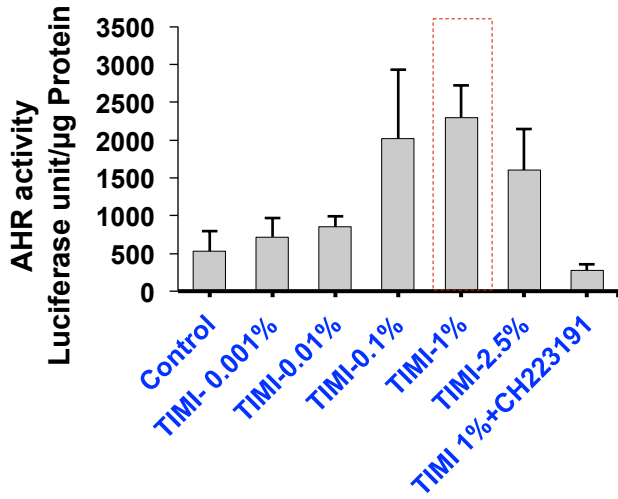
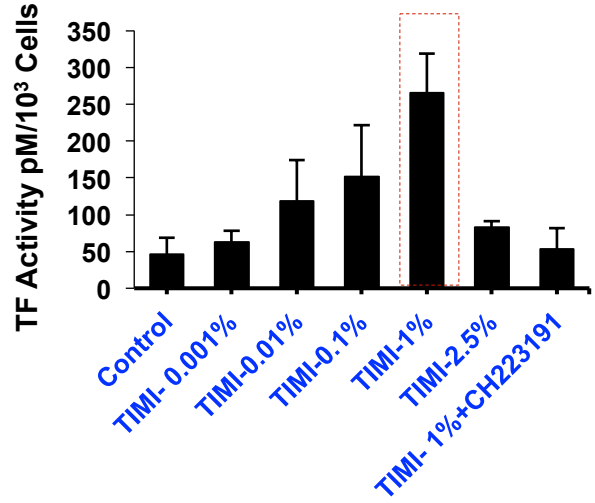
(A). Immunoblotting of the endothelial marker VE cadherin in HUVEC (4 passages), HUVEC-tert (15 passages). Note the absence of expression in negative controls NIH3T3 (mouse embryo fibroblastic cell line), and HK-2 (human kidney cortex/proximal tubule epithelial cell line). The lysates were probed for VE-cadherin (an endothelial marker) and Actin served as a control.

(B). *In vitro* angiogenesis assay of HUVEC and HUVEC-tert cells. Cells were seeded in a growth factor poor Matrigel™-coated 96 well plate and analyzed for tube formation after 24 hours of culture. Representative image of three independent experiments is shown. The tube formation is a biological assay, which supports the retention of endothelial feature of HUVEC-tert cells.

(C). Tube lengths were quantified using Image J. Mean of two separate experiments performed in triplicate is shown. Six images were evaluated in each well. Student's t-test with Bonferroni's correction was performed to determine statistical significance. Error bars = SEM. The significant difference in the tube length was observed between these cells.

(D). Standard curve of vSMC numbers in MTT assay. Serial dilutions of vSMCs counted using a cell counter were seeded in in 6 wells of 96-well plate done in two duplicate sets. One set was subjected to MTT assay using Alamar Blue® after 24 hours of seeding and other set was trypsinized and counted using a cell counter. The average of number of cells in 6 wells (X-axis) was plotted against the average absorbance values of Alamar Blue at 570nm (Y-axis). Resulting regression equation (inset) was used to determine the number

of cells in subsequent MTT assays. The number of cells was used to normalize the surface procoagulant TF activity assay.

A**B****C****D**

Supplementary Figure 7. Determining the optimum serum concentration for the DAC and TIMI-II samples.

A set of five randomly selected subjects from DAC (panels **A and B**) and TIMI-II (panels **C and D**) were used to titrate the optimal concentration of serum for maximal signal detection in AHR (panels A and C) and TF (panels B and D) activity assays. Control: serum from healthy subjects. CH223191: AHR inhibitor. The activity assays were performed in three independent experiments each done in duplicate. An average of reading of AHR and TF activities represented in luciferase unit/ μg protein and TF activity pM/ 10^3 cells, respectively, are shown. The values in box indicate the serum concentration used for both the assays in these two trials.

SIGNIFICANCE STATEMENT

CKD is a strong risk factor for thrombosis. Previously, animal studies have shown that uremic solutes mediate this event through the activation of Aryl Hydrocarbon Receptor (AHR) and tissue factor (TF), thus, defining a uremic thrombosis axis. In this study, its human relevance is examined using data collected from two distinct clinical trials. In line with the animal studies, the analysis on 850 sera samples showed a significant correlation of a set of uremic solutes, AHR and TF activities with the thrombotic events. This human validation supports further studies to explore this novel axis as a uremic thrombosis biomarker and to test its contribution in other diseases characterized by thrombosis.